Article

Current Biology

Membrane-associated NRPM proteins are novel suppressors of stomatal production in *Arabidopsis*

Graphical abstract

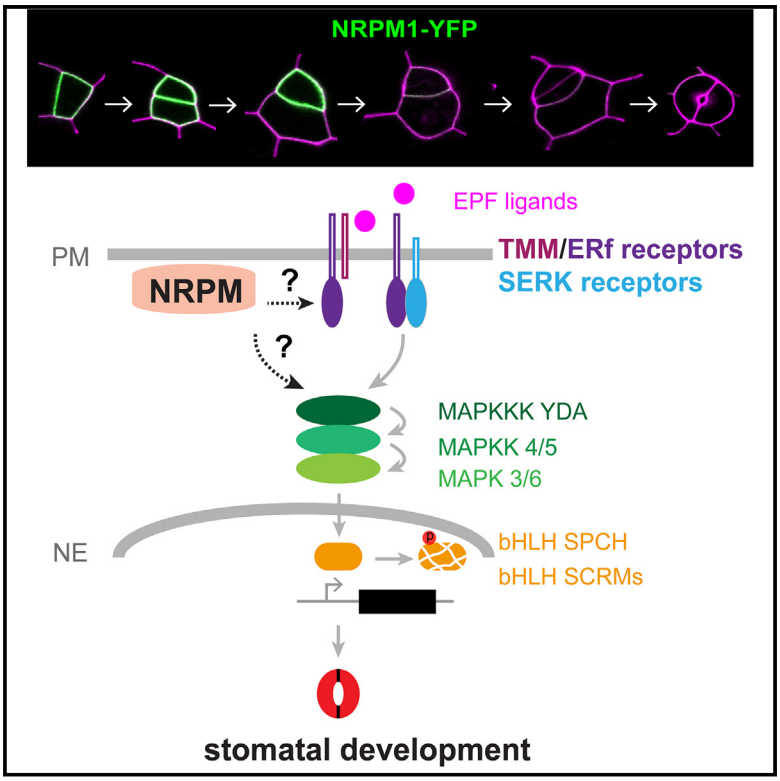

Highlights

- *NRPM1* is highly expressed during stomatal asymmetric cell division
- NRPMs are four novel stomatal repressors functioning inside the plasma membrane
- Mutating *NRPM* genes attenuates the plasma membrane localization of ERECTA
- NRPMs function upstream of the MAPKKK YDA in stomatal development

Authors

Xueyi Xue, Lu Wang, Aobo Huang, ..., Jian-Kang Zhu, Huiling Xue, Juan Dong

Correspondence

xyxue@cau.edu.cn (X.X.), dong@waksman.rutgers.edu (J.D.)

In brief

External signaling pathways heavily influence plant development in *Arabidopsis*. Xue et al. identify the NRPM proteins as novel signaling molecules at the plasma membrane that suppress stomatal production. This underscores an unrecognized regulatory module between the membrane receptors and the MAPK cascade.

Xue et al., 2024, Current Biology *34*, 881–894
February 26, 2024
https://doi.org/10.1016/j.cub.2024.01.052

CellPress

Current Biology

CellPress

Article

Membrane-associated NRPM proteins are novel suppressors of stomatal production in *Arabidopsis*

Xueyi Xue,[1,2,*] Lu Wang,[3] Aobo Huang,[1] Zehao Liu,[4] Xiaoyu Guo,[1] Yuying Sang,[5] Jian-Kang Zhu,[5,7] Huiling Xue,[4] and Juan Dong[1,6,8,*]

[1]The Waksman Institute of Microbiology, Rutgers, the State University of New Jersey, Piscataway, NJ 08854, USA
[2]Sanya Institute of China Agricultural University, Sanya 572025, China
[3]College of Life Sciences, Qingdao University, Qingdao 266071, China
[4]College of Animal Science and Veterinary Medicine, Shenyang Agricultural University, Shenyang 110866, China
[5]Shanghai Center for Plant Stress Biology, Chinese Academy of Sciences, Shanghai 201602, China
[6]Department of Plant Biology, Rutgers, the State University of New Jersey, New Brunswick, NJ 08901, USA
[7]Present address: Institute of Advanced Biotechnology and School of Life Sciences, Southern University of Science and Technology, Shenzhen 518055, China
[8]Lead contact
*Correspondence: xyxue@cau.edu.cn (X.X.), dong@waksman.rutgers.edu (J.D.)
https://doi.org/10.1016/j.cub.2024.01.052

SUMMARY

In *Arabidopsis*, stomatal development and patterning require tightly regulated cell division and cell-fate differentiation that are controlled by key transcription factors and signaling molecules. To identify new regulators of stomatal development, we assay the transcriptomes of plants bearing enriched stomatal lineage cells that undergo active division. A member of the novel regulators at the plasma membrane (NRPM) family annotated as hydroxyproline-rich glycoproteins was identified to highly express in stomatal lineage cells. Overexpressing each of the four *NRPM* genes suppressed stomata formation, while the loss-of-function *nrpm* triple mutants generated severely overproduced stomata and abnormal patterning, mirroring those of the *erecta* receptor family and MAPKKK *yoda* null mutants. Manipulation of the subcellular localization of NRPM1 surprisingly revealed its regulatory roles as a peripheral membrane protein instead of a predicted cell wall protein. Further functional characterization suggests that NRPMs function downstream of the EPF1/2 peptide ligands and upstream of the YODA MAPK pathway. Genetic and cell biological analyses reveal that NRPM may promote the localization and function of the ERECTA receptor proteins at the cell surface. Therefore, we identify NRPM as a new class of signaling molecules at the plasma membrane to regulate many aspects of plant growth and development.

INTRODUCTION

Stomata are microscopic pores in the epidermis of the aerial organs of a plant. Each stomatal pore is surrounded by a pair of guard cells that, through turgor-driven cell expansion, regulate gas exchange and water transpiration between plants and the environment. Stomatal development and patterning in the dicot model plant *Arabidopsis* have been well studied and provide an excellent system for studying cell polarity, cell division, cell-fate transition, and cell-fate differentiation.[1,2]

The progression of stomatal differentiation in *Arabidopsis* requires successive activities of three basic helix-loop-helix (bHLH) transcription factors, SPEECHLESS (SPCH), MUTE, and FAMA.[3,4] Another two bHLH transcription factors, SCREAM (SCRM) and SCRM2, redundantly form heterodimers with SPCH, MUTE, and FAMA, respectively, to drive the three successive steps of cell-fate transition in stomatal development.[5] The mitogen-activated protein kinase (MAPK) cascades are critical signaling pathways that regulate diverse cellular processes by transmitting extracellular stimuli to intracellular machinery.[6–8] Stomatal development and patterning in *Arabidopsis* are also controlled by a canonical MAPK cascade, including the MAPK kinase YODA (YDA), MAPK kinase 4 and 5 (MKK4/5), and MAPK 3 and 6 (MPK3/6).[9–11] Biochemical and genetic analyses certified a crucial role of this YDA-MKK4/5-MPK3/6 cascade in suppressing stomatal production through phosphorylation-mediated degradation of SPCH and SCRM.[4,12] In addition, recent studies revealed that SCRM as a scaffold brings SPCH approximately to MPK6, improving the efficiency of phosphorylation and subsequent degradation of SPCH.[13]

Plants have evolved the use of the secreted epidermal patterning factor (EPF) peptides to prevent neighboring cells from entering the stomatal fate. The EPF peptide ligands are perceived by the cell surface leucine-rich repeat receptor-like proteins (LRR-RLPs) and kinases (RLKs), including TOO MANY MOUTHS (TMM), the ERECTA family (ER-f), and the somatic embryogenesis receptor kinase (SERK) family.[14–18] Activated RLP/RLK signaling triggers the downstream YDA-MKK4/5-MPK3/6 signaling cascade, which

then regulates the substrate levels or activities, such as SPCH.[9–11] However, how the LRR-RLP/RLK complexes transmit the signal to the MAPK cascade is still unclear.

In this study, based on the transcriptome profiling data, we identified a group of proteins annotated as hydroxyproline-rich glycoproteins (HRGPs) with the founding member highly expressed in the dividing stomatal lineage cells. Mutating three of the four closely related *HRGP* genes led to overly proliferative stomatal lineage cells, as well as broad defects in growth and development, to some extent resembling those of the *yda* and *erecta* family mutants.[9,19] In plants, HRPGs are known as a superfamily of plant cell wall proteins that function widely in plant growth and development.[20,21] However, how they function remains almost unknown. Here, we found that the novel regulators at plasma membrane (NRPM) family of these putative HRGPs function inside of the plasma membrane (PM) and negatively regulate stomatal production downstream of the peptide ligands EPF1/2, upstream of YDA, and partially through the ERECTA receptor.

RESULTS

RNA-seq-based identification of new regulators in stomatal ACD

In *Arabidopsis*, the bHLH transcription factor SPCH determines the initiation of stomatal lineage cells.[22] Overexpression of a truncated SPCH variant, SPCHΔ49 that is insensitive to MAPK-triggered protein phosphorylation for degradation, produces excessive stomatal lineage cells in the leaf epidermis.[4] Stomatal asymmetric cell division (ACD) is controlled by the scaffold protein BREAKING OF ASYMMETRY IN THE STOMATAL LINEAGE (BASL) that polarizes at the cortical region of the precursor cells to drive division orientation and specify distinct daughter-cell fates.[23–25] In the absence of *BASL*, the stomatal lineage divisions largely lost their physical and fate asymmetries.[23] To identify new regulators in stomatal ACD, we conducted a transcriptomic analysis using young plants overexpressing *SPCHΔ49* (driven by the ubiquitous 35*S* promoter) that produce excessive stomatal lineage cells and overexpressing *SPCHΔ49* in *basl*-2 mutants that produce a comparative amount of stomatal lineage cells but less asymmetric in divisions (Figure 1A). We expected that stomatal ACD regulators would show high expression levels in *SPCHΔ49* but reduced levels in *SPCHΔ49;basl-2* and wild-type (WT) plants.

To perform genome-wide RNA-seq analyses, total RNAs were extracted and purified from seedlings of WT, *SPCHΔ49*, and *SPCHΔ49;basl-2* at 12 days post-germination (dpg). The heatmap displaying differentially expressed genes (DEGs) clustered with similar expression patterns suggested that the plants overexpressing *SPCHΔ49* are most distinct from the WT plants and moderately different from *SPCHΔ49;basl-2* (Figure 1B). Through pairwise comparison, a total of 1,949 DEGs (transcript per million [TPM] > 10, $|b| \geq 0.692$, $q < 0.05$) were identified, and upregulated/downregulated DEGs were plotted by Venn diagrams (Figure 1C; gene lists in Data S1). Genes known to regulate stomatal development, such as *SPCH*, *MUTE*, *SCRM*, and other regulators involved in signal transduction (the peptide ligands, membrane receptors, and cytoplasmic kinases), were highly enriched in the *SPCHΔ49* overexpression plants (Figure S1A). As we were interested in the genes differentially expressed between *SPCHΔ49* and *SPCHΔ49;basl*-2, the 172 upregulated DEGs in *SPCHΔ49* were subjected to the gene ontology (GO) analysis. We found that these genes are mostly enriched in the processes of cell cycle, stomatal complex development, cell division, cell wall organization, mitotic apparatus, ACD, etc. (Figure 1D; Data S1). We selected candidate genes possibly involved in membrane dynamics, signal transduction, and cytoskeletal organization for promoter activity tests. Indeed, we found many promoters, such as that of *AT4G26660* (encodes a kinesin-like protein) and *AT1G53140* (encodes a dynamin-related protein), showed strong and specific activities in the stomatal lineage cells (Figures S1B and S1C). Furthermore, twenty intersection DEGs were commonly identified to show higher transcript levels among the three pairs of comparisons (Figure 1C). Among them, besides *SPCH* itself, genes encoding transcriptional factors WRKY50, NAC035, and NAC041, as well as known stomatal genes such as *TMM*, *ETC3 (ENHANCER OF TRY AND CPC 3)*, and *BHP* (*BLUE LIGHT-DEPENDENT H+-ATPASE PHOSPHORYLATION*) were identified. The eight genes with unknown functions (labeled with AGI) were also isolated (Figure 1E). Particularly, *AT4G25620* was found to be highly expressed in the actively dividing meristemoids in the *scrm-D;mute* mutants (Figure S1D).[26]

We further screened the candidate genes by creating overexpression plants and/or the loss-of-function mutants (T-DNA insertional or CRISPR-Cas9-mediated mutagenesis). Among the tested candidates, AT4G25620 became the top priority because of the strong phenotypes in stomatal development associated with altered gene activity in *Arabidopsis* (see below).

NRPMs are expressed in the stomatal lineage cells

AT4G25620 encodes an HRGP with unknown functions and is active exclusively in the stomatal lineage cells (Figure 2A). AT4G25620 belongs to a four-member family (Figure 2B). We first examined the subcellular localization by transiently expressing yellow fluorescent protein (YFP)-tagged members in the *Nicotiana benthamiana* epidermal cells. Surprisingly, all four proteins are distributed along the PM (Figure S1E). This observation was in striking contrast to the original annotation that the HRGPs are usually located in the cell wall.[27] As their location was later determined to be the PM (detailed below), AT4G25620 and the other family members were accordingly named as novel regulators at the plasma membrane (NRPM) from here on (Figure 2B).

To characterize their functions, we first assayed the promoter activity of each *NRPM* gene. We found that, except for *NRPM3* (*AT1G63720*), which appeared to be expressed in the mesophyll cells, all the other three *NRPM* promoters show activities in the epidermal cells (Figure S1F). Furthermore, compared with the broad expression pattern of *NRPM2* (*AT5G52430*) in the leaf epidermis, *NRPM1* and *NRPM4* (*AT1G76660*) were more restricted to the stomatal lineage (Figure S1F). The endogenous protein localization of NRPMs was further assayed in *Arabidopsis* plants by expressing NRPM-YFP driven by the respective native promoter. Consistent with the transient protein-expression data, all three NRPM proteins were localized to the PM in *Arabidopsis* plants (Figure 2C). As NRPM3 is absent from the leaf epidermal cells (Figure 2C), we examined whether and how NRPM1/2/4 proteins are differentially expressed in the stomatal lineage cells. Interestingly, NRPM1-YFP is specifically expressed in the early

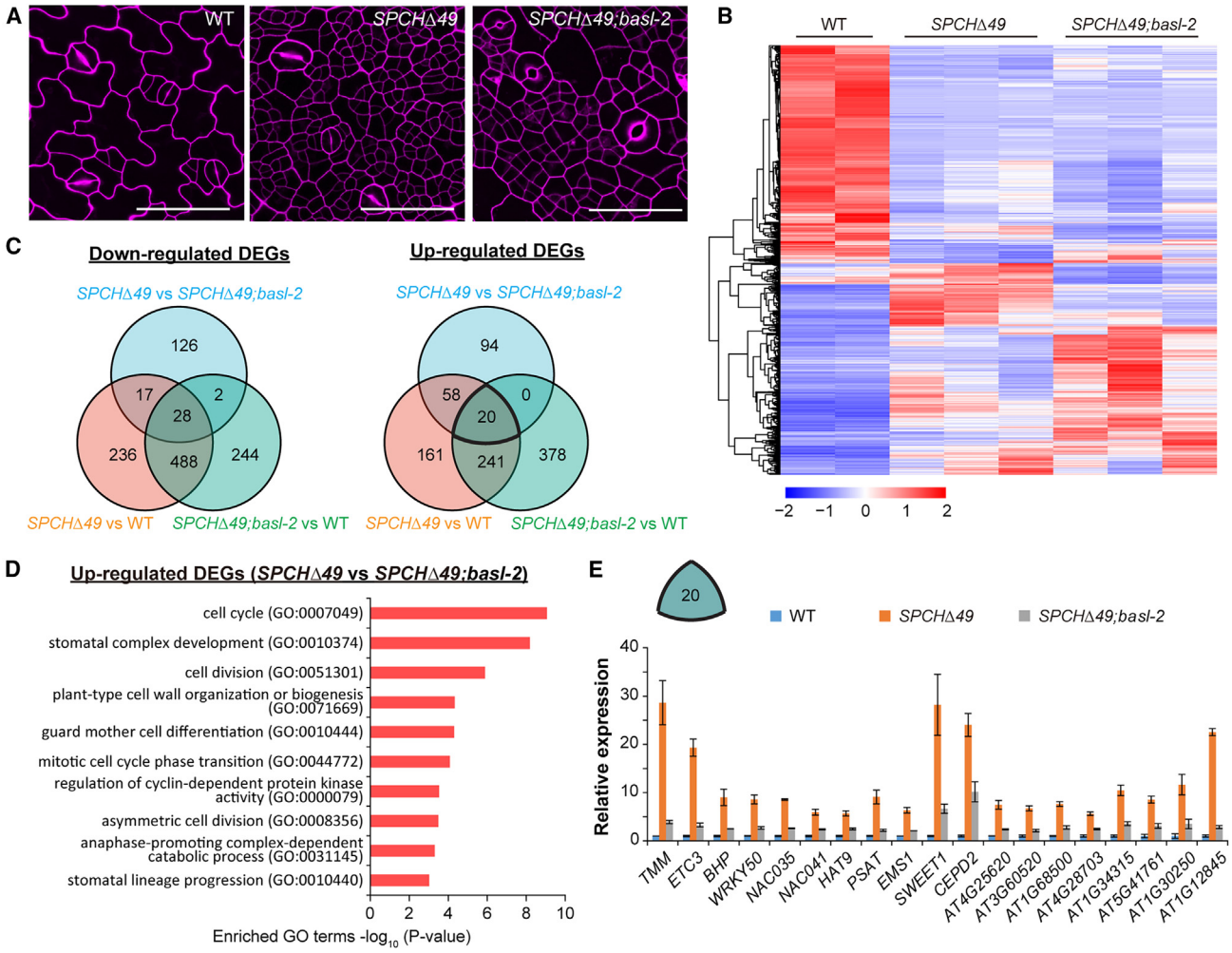

Figure 1. Identification of genes differentially expressed in actively dividing stomatal lineage cells

(A) Confocal images show epidermal cell patterns on cotyledons at 3 days post-germination (dpg) in wild type (WT), *SPCHΔ49*, and *SPCHΔ49;basl-2*. *SPCHΔ49*, overexpression of a phospho-deficient SPCH variant in wild type that induces the overproduction of stomatal lineage cells. In *SPCHΔ49;basl-2* mutants, these divisions are less asymmetric. Cell outlines were stained with propidium iodide (PI, magenta). Scale bars, 50 μm.

(B) Differentially expressed genes (DEGs) in WT, *SPCHΔ49*, and *SPCHΔ49;basl-2*. Total RNAs were isolated from 12-dpg seedlings of indicated genotypes for transcriptomic analysis. Two biological replicates for WT and three biological replicates for *SPCHΔ49* and *SPCHΔ49;basl-2* were used for this experiment.

(C) Venn diagrams show DEGs downregulated (left) and upregulated (right) when the two genotypes were compared as indicated.

(D) GO-term enrichments of upregulated DEGs in *SPCHΔ49* vs. *SPCHΔ49;basl-2*.

(E) Relative transcript levels of the 19 upregulated DEGs at the intersection in (C) (SPCH excluded). The transcript levels of each gene in WT were normalized to 1. Values are mean ± SEM (n = 2 or 3).

See also Figure S1 and Data S1.

stomatal lineage cells, i.e., the meristemoid mother cells (MMCs) and meristemoids (Figure 2D); contrastingly NRPM4-YFP is preferentially expressed in the late staged cells, such as guard mother cells (GMCs) and young guard cells (GCs) (Figure 2D). On the other hand, NRPM2-YFP is expressed in almost all epidermal cells, except for the mature GCs (Figures 2C and 2D). Thus, despite their preferential cell-type expression patterns, all three genes, *NRPM1*, *NRPM2*, and *NRPM4*, could contribute to regulating stomatal development.

NRPMs suppress stomatal production at the PM

Since no transmembrane domains were predicted by DeepTMHMM[28] and the proteins were annotated as HRGPs, the localization of NRPMs at the PM was a surprise. To confirm that NRPMs indeed associate with the PM, we conducted the plasmolysis assay, in which plants were treated with 20% (w/v) sucrose for 20 min. As shown in Figure 2E, the NRPM1/2/4-YFP signals retracted with the PM upon plasmolysis, but no significant signals were detected in the cell walls, suggesting that NRPMs are indeed peripheral membrane proteins.

To study their functions, we overexpressed each of the four *NRPM* genes under the control of the ubiquitous *CaMV 35S* promoter in WT *Arabidopsis* plants (Figure S2A). Interestingly, once overexpressed, all four NRPM members can suppress stomata development (Figures 3A–3C), as suggested by the stomatal index (% of stomatal number over total number of epidermal cells).

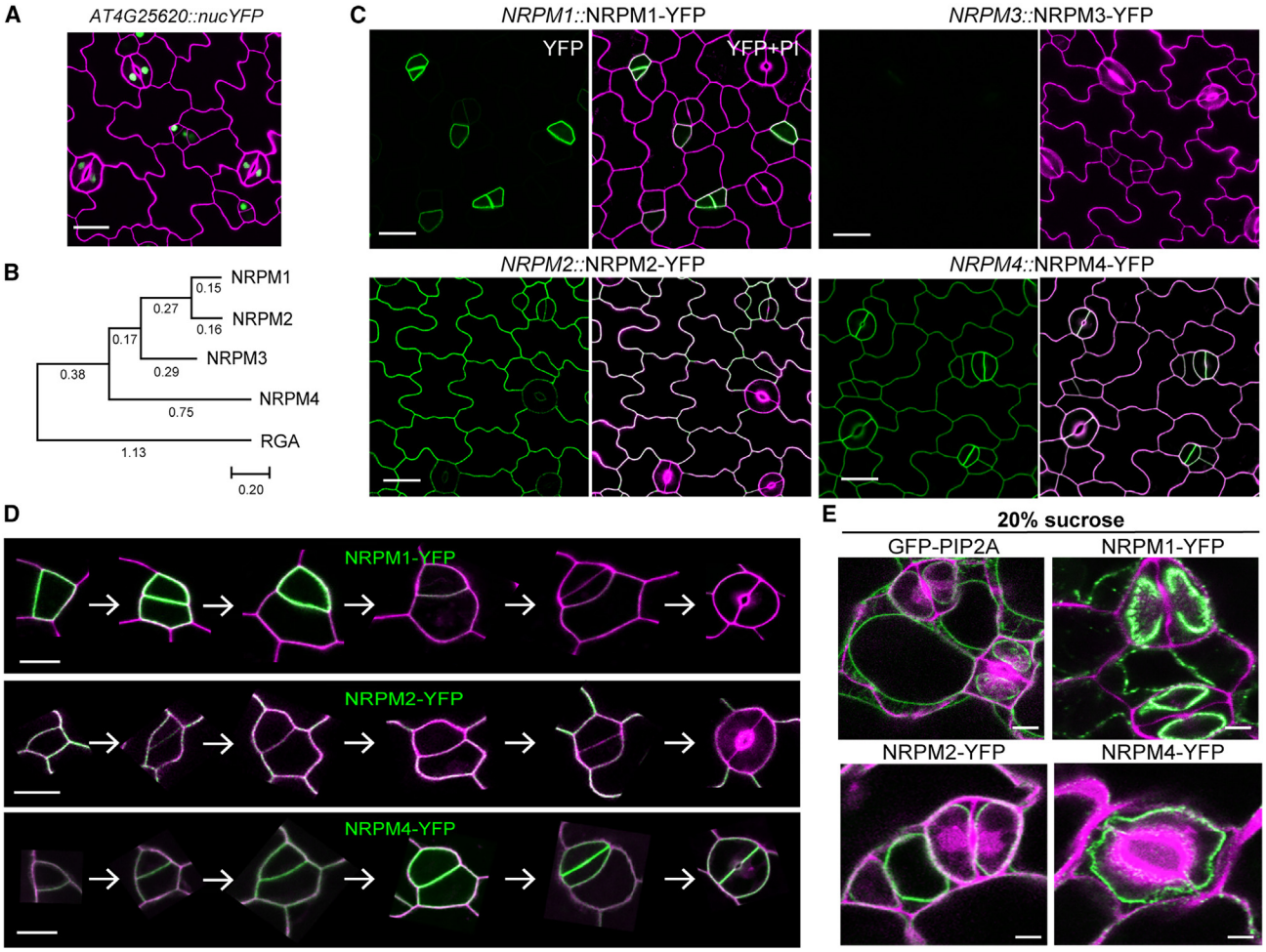

Figure 2. NRPMs are mainly expressed in the leaf epidermis

(A) Activity of the *NRPM1* promoter (*AT4G25620*) is detected high in stomatal lineage cells. Cell outlines were stained with PI (magenta). Scale bars, 20 μm.

(B) The phylogenetic tree of the *Arabidopsis* NRPM family. A neighbor-joining tree with distance shows the evolutionary relationships between NRPM members. REPRESSOR OF GA (RGA, AT2G01570) serves as the outgroup to anchor the tree.

(C) Expression patterns of the four *NRPM* genes in 3-dpg cotyledons. NRPM-YFP (green) was driven by the respective native promoter. NRPM1 is active in meristemoid mother cells (MMCs) and meristemoid; NRPM2 accumulates in all epidermal cells except for mature guard cells; no NRPM3 is expressed in epidermal cells; NRPM4 is present in all epidermal cells. Scale bars, 20 μm.

(D) Differential expression patterns of NRPM1/2/4-YFP protein (green) during stomatal development. Representative images for each stage were selected based on cell morphology. NRPM1 is active before guard mother cells (GMCs). NRPM2 shows low to no expression in differentiating guard cells. NRPM4 shows elevated expression levels in GMC and young guard cells. Cell outlines were stained with PI. Scale bars, 20 μm.

(E) Plasmolysis assays show that NRPM1/2/4-YFP proteins (green) are associated with the plasma membrane that is detached from the cell wall after the seedlings were treated with 20% sucrose. Control: GFP-PIP2A (plasma membrane intrinsic protein 2A), an integral membrane protein (green). Scale bars, 5 μm. See also Figure S1.

In addition, overexpression of these *NRPM* genes caused general defects in plant growth and development, such as stunted stature and spiral rosette leaves (Figure 3A). To further test whether NRPMs function from outside or inside of the PM, we engineered the WT NRPM1 protein by adding a myristoylation (myr) lipid modification sequence[29] that helps to tether the target protein to the PM or by adding the signal peptide (sp) of an Extensin protein[30] that directs the target protein to the cell wall (Figure 3D and sequence in Figure S2B). As anticipated, myr-NRPM1 was found exclusively along the PM, whereas sp-NRPM1 was distributed to the endomembrane compartments and the cell walls (Figure 3D). Interestingly, myr-NRPM1-YFP maintained the ability to suppress stomata formation, whereas sp-NRPM1-YFP failed to induce this phenotype (Figure 3E), strongly suggesting that NRPMs may function at the inner side of the PM to regulate stomatal development.

Loss-of-function *nrpm* mutants show stomatal overproduction

To further characterize the NRPMs' function in stomatal development, we collected individual *NRPM* T-DNA insertional mutants (Figure S3A). No visible phenotypes were observed in the single mutants under optimal growth conditions (Figure S3B). As the expression of *NRPM3* was not detected in the epidermal

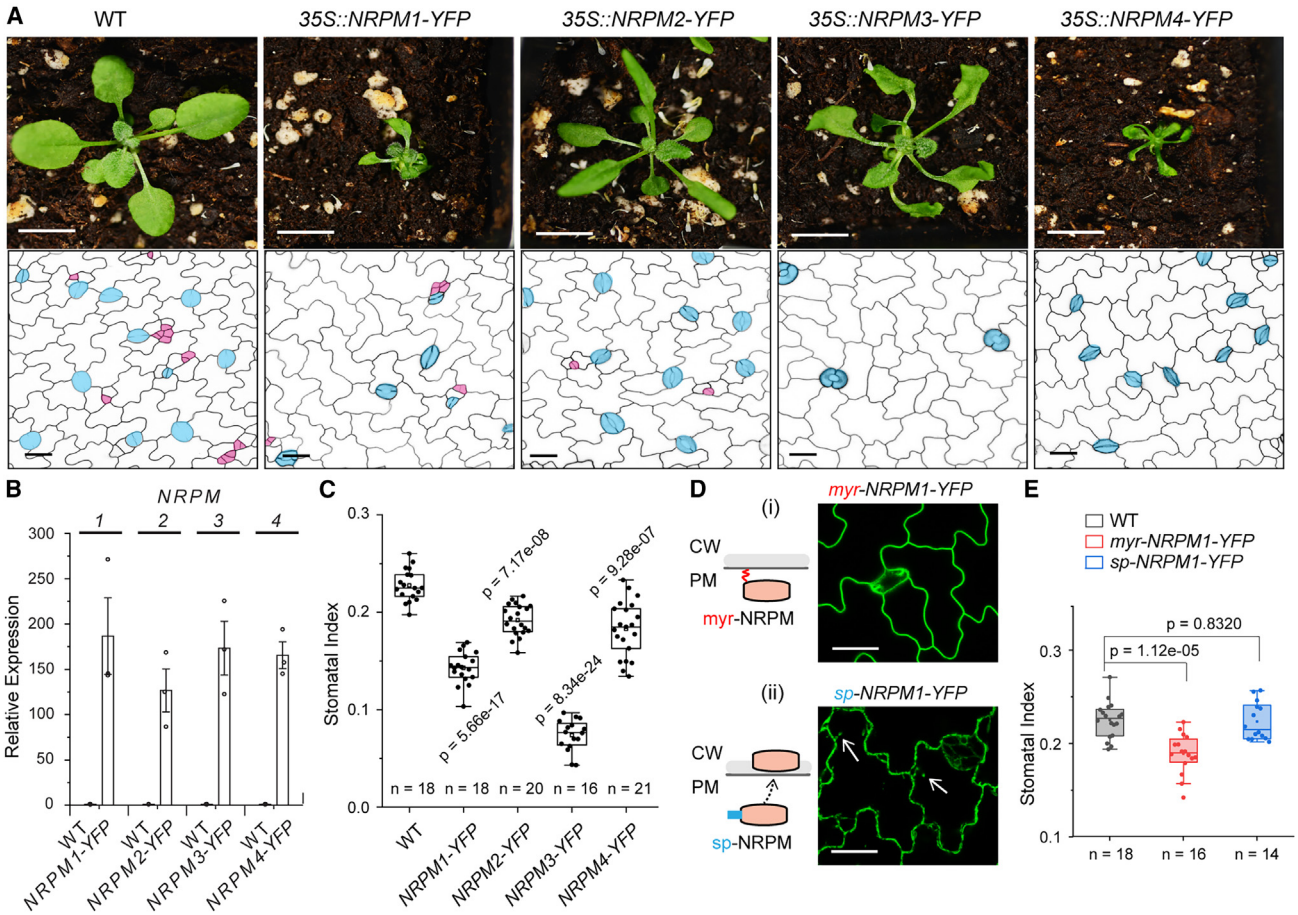

Figure 3. Overexpression of NRPM suppresses stomata production at the membrane periphery

(A) Representative images show that overexpression of NRPMs reduces stomatal production and disturbs plant growth and development. Upper: 3-week-old plants under normal growth conditions. Scale bars, 1 cm. Lower: stomatal development and patterning in the adaxial side of 3-dpg cotyledons. Stomatal guard cells and dividing cells are colored in cyan and pink, respectively. Two independent lines for each transgene were established, and expression levels are shown in Figure S2A. WT: Columbia-0 plants expressing *ML1::YFP-RCI2A* (the transmembrane protein RCI2A driven by the epidermal specific *ML1* promoter). Scale bars, 20 μm.

(B) Quantitative PCR analyses show transcript levels of each *NRPM* in the overexpression plants shown in (A). The transcript levels of each *NRPM* in WT were normalized to 1. Values are mean ± SEM (n = 3).

(C) Quantification of stomatal index in 5-dpg cotyledons of indicated plants. Student's unpaired t tests were used to calculate the two-tailed p value when compared with the wild type.

(D) Confocal images show the localization of two engineered NRPM1-YFP proteins (green). The addition of a myristoylation (myr) peptide sequence targets NRPM1 to the inner leaflet of the plasma membrane, whereas the addition of an Extensin signal peptide (sp) drives NRPM1 to the secretory pathway. Arrows mark the *trans*-Golgi network-like structures as anticipated. Scale bars, 20 μm.

(E) Quantification of stomatal index in 5-dpg cotyledons of the transgenic plants shown in (D). The myr-NRPM1-YFP suppresses stomata formation, whereas the apoplastic sp-NRPM1-YFP fails to do so. Student's unpaired t tests were used to calculate two-tailed p values. Boxes in (C) and (E) show first and third quartiles with mean (square) and median (line). Whiskers extend to 1.5 × interquartile range (IQR) from the first and third quartile. n, number of cotyledons analyzed. See also Figure S2.

cells, we generated double mutants among *nrpm1*, *nrpm2*, and *nrpm4*, in which *nrpm1* and *nrpm4* appeared to be null and *nrpm2* was a knockdown mutant (Figure S3C). The double mutants, *nrpm1;2* and *nrpm2;4*, were first isolated, but we did not detect observable stomatal or other growth defects (Figure S3D), except that *nrpm2;4* mutants produce shorter siliques with fewer seeds that can be complemented by expressing NRPM2-YFP driven by the native promoter (Figure S3E). However, we failed to obtain a *nrpm1;4* double mutant, although *NRPM1* and *NRPM4* are located at two different chromosomes. In fact, we found that any individuals with the genotype of *nrpm1*−/−;*nrpm4*−/+ or *nrpm1*−/+;*nrpm4*−/− were absent from the F2 population of *nrpm1*−/− crossed with *nrpm4*−/− (Table S1). Therefore, we speculated that missing more than three copies from these two *NRPM* genes (1 and 4) would cause embryonic lethality, which is further supported by seed abortion phenotype observed in the siliques of a *nrpm1*−/+;*nrpm4*−/+ plant (Figure S3F). Also, the promoter activities of both *NRPM1* and *NRPM4* were detected in developing seeds, i.e., the endosperm region around the micropylar (arrows in Figure S3G).

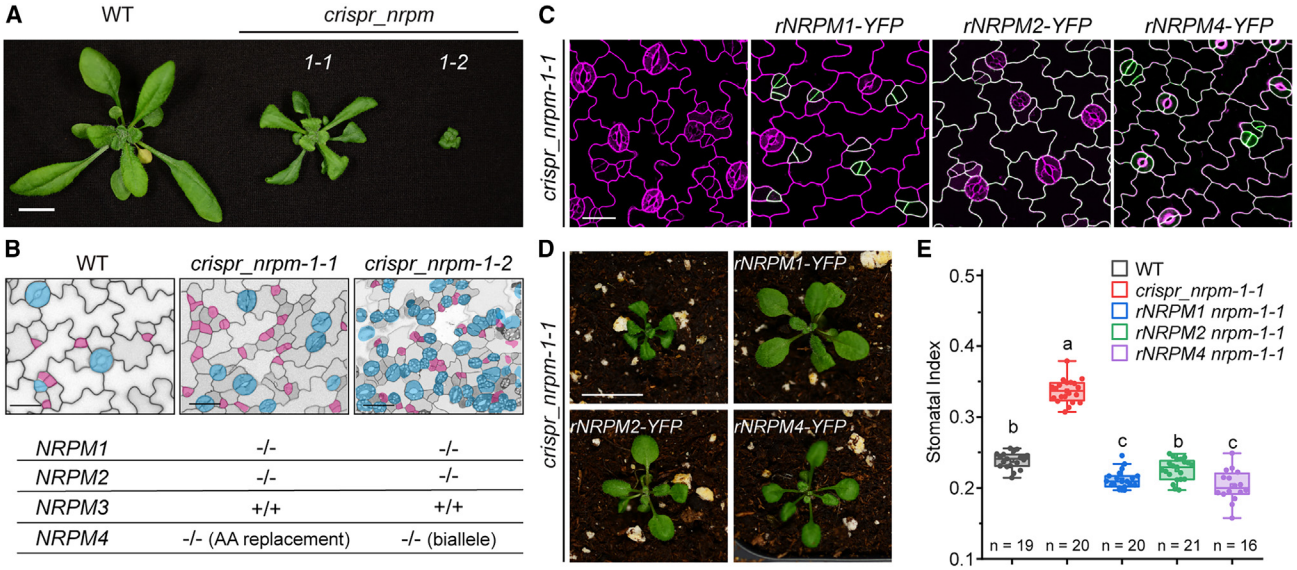

Figure 4. Mutations in *NRPMs* result in severely overproduced stomata

(A) Mutating *NRPM1/2/4* interferes with plant growth and development. Mutant plants (*crispr_nrpm-1-1* moderate and *crispr_nrpm-1-2* strong) were identified in the progenies of a single T1 transformant carrying CRISPR-Cas9-mediated mutagenesis of *NRPM1/2/4*. WT: Col-0 plants expressing *ML1::mCherry-RCI2A* (21 dpg). The *crispr_nrpm* plants were created in the same background. Scale bars, 1 cm.

(B) Stomatal phenotypes (upper) and genotypes (lower) of *crispr_nrpm-1-1 and crispr_nrpm-1-2* mutants. Specific mutations are provided in Figure S4A. Stomata guard cells and small dividing cells are colored in cyan and pink, respectively. Scale bars, 25 μm.

(C) Expression of CRISPR-resistant *NRPM1/2/4* (*rNRPM*)-YFP transgene (green) largely rescued stomata defects in *crispr_nrpm-1-1* plants. *rNRPM-YFP* carrying CRISPR-off-target-synonymous mutations driven by the native promoter was introduced into *crispr_nrpm-1-1*. Confocal images with cell outlines marked by mCherry-RCI2A (magenta) were captured from 3-dpg cotyledons. Scale bars, 20 μm.

(D) Recovery of plant growth defects in *crispr_nrpm-1-1* was observed by expressing the native promoter-driven *rNRPM1/2/4*. Representative images show 16-dpg plants. Scale bars, 1 cm.

(E) Quantification of stomatal index in the adaxial side of 5-dpg cotyledons of *crispr_nrpm-1-1* and *rNRPM1/2/4* complementation lines shown in (D). Boxes show the first and third quartile with mean (square) and median (line). Whiskers extend to 1.5 × IQR from first and third quartile. Letters (a, b, and c) indicate significantly different means at $p < 0.05$ (one-way ANOVA). n, number of cotyledons analyzed.

See also Figures S3 and S4 and Table S1.

Therefore, strong T-DNA insertional alleles of *nrpm* mutations, in particularly the combined effect of *nrpm1* and *nrpm4*, could lead to detrimental failures in embryo development, which greatly interfered with our ability to assay their functional contribution in post-embryonic processes, including stomatal development.

To study the function of NRPM during stomatal development, we took advantage of the CRISPR-Cas9-mediated genome editing that allows the creation of weak alleles, such as short deletions or replacements. We assembled four guide RNAs in one construct with each guide RNA targeting one of the four *NRPM* genes in the exon region (Figure S3A) and transformed it into WT plants. Interestingly, we identified three categories of plants segregating from one mother plant that show (1) WT-looking, (2) mildly disturbed (*crispr_nrpm-1-1*), and (3) severely disturbed growth (*crispr_nrpm-1-2*), respectively (Figure 4A). Furthermore, the severity of overall growth phenotypes was mirrored by stomatal defects in these mutants (Figure 4B). Genotyping data demonstrated that we successfully generated mutations in *NRPM1/2/4* but not in *NRPM3* (summarized in Figure 4B and detailed in S4A). Specifically, both *crispr_nrpm-1-1* (moderate) and *crispr_nrpm-1-2* (strong) carry homozygous early terminations in both *NRPM1* and *NRPM2*. Mutating *NRPM4* appeared to be most influential to the phenotypes because the moderate mutant *crispr_nrpm-1-1* harbors an in-frame replacement, resulting in 13 amino acids (aa) replacement of the original 3 aa, whereas the strong mutant *crispr_nrpm-1-2* contains biallelic early terminations in *NRPM4* (Figures 4B and S4A). Thus, results from our CRISPR-Cas9-mediated mutagenesis revealed the redundant role of *NRPM1, 2*, and *4* in suppressing stomatal production and enforcing stomatal patterning.

Next, we performed complementation assays to confirm the functional relevance of *NRPMs* in plant development. Since we were unable to obtain CRISPR-Cas9-free individuals from the *crispr_nrpm-1* population, we expressed the *NRPM* variants (*rNRPMs*) that carry synonymous mutations (Figure S4B) that are resistant to the CRISPR-Cas9-mediated mutagenesis in the *crispr_nrpm-1-1* mutants. As expected, the rNRPM1/2/4-YFP protein fusions driven by their own promoter recapitulated the native protein localization at the PM (Figure 4C). Importantly, all three constructs efficiently complemented the *crispr_nrpm-1-1* mutant phenotypes in stomatal development and overall growth (Figures 4D and 4E). Thus, *NRPM1, 2*, and *4* redundantly regulate many aspects of plant growth and development.

Functional connection between NRPM and ER-f in stomatal development

Among the T2 population of CRISPR-Cas9-generated *nrpm* mutants, we observed varying developmental defects reminiscent

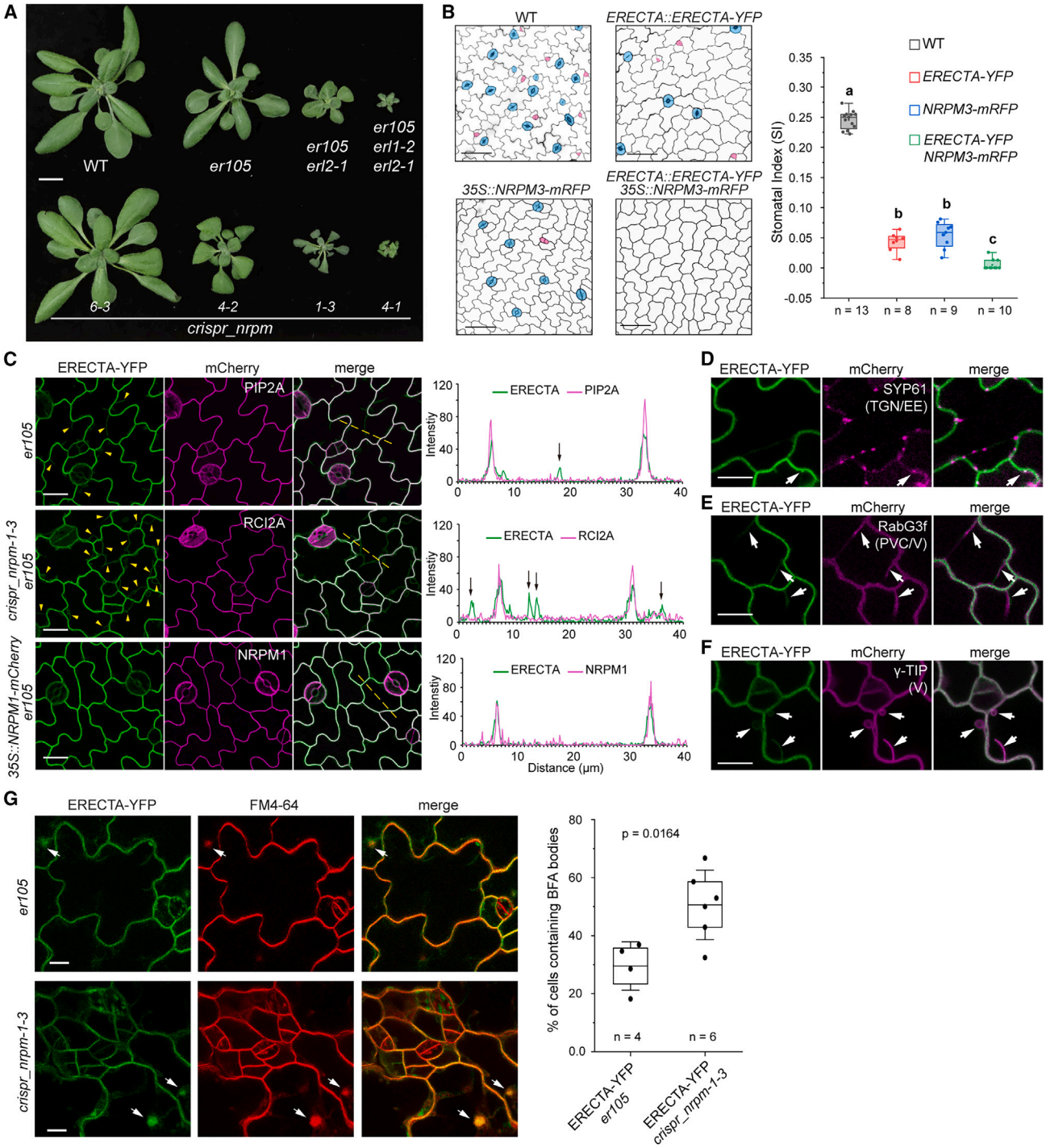

Figure 5. NRPMs promote the plasma membrane localization of the ERECTA receptor

(A) Developmental defects observed in the *crispr-nrpm* mutants mirror those identified in the *erecta* family mutants (24 dpg). Specific *NRPM* mutations in different *crispr_nrpm* alleles are provided in Figure S4A. Scale bars, 1 cm.

(B) Stomatal phenotypes (5 dpg) generated by the elevated expression of *ERECTA* and *NRPM3* in the wild-type plants. Note, enhanced phenotype was observed in plants co-expressing *ERECTA::ERECTA-YFP* and *35S::NRPM3-mRFP*. Stomatal guard cells and lineage cells are colored in cyan and pink, respectively. Scale bars, 50 μm. Histograms on the right show the quantification of stomatal index in the adaxial side of 5-dpg cotyledons. Boxes show first and third quartile with mean (square) and median (line). Whiskers extend to 1.5 × IQR from the first and third quartile. Letters (a, b, and c) indicate significantly different means at $p < 0.05$ (one-way ANOVA). n, number of cotyledons analyzed.

(C) Confocal images show enhanced and lowered internalization of ERECTA-YFP (green) in *crispr_nrpm* mutants and *NRPM1* overexpression plants (3 dpg), respectively. Yellow arrowheads: internalized signals of ERECTA-YFP. Note the difference in different genetic backgrounds. Cell outlines (magenta) were

(legend continued on next page)

of sequentially knocking out the *ER-f* members (Figures 5A and S5A). Moreover, the phenotypic severity of *nrpm* mutants appeared to be associated with the mutation features of *nrpm4*, while *nrpm1* and *2* were all early terminations (Figure S4A). For example, the weak mutant *crispr_nrpm-4-2* showing phenotypes at the *er105* level contains *nrpm4*−/+ (early termination, heterozygous), and the moderate mutant *crispr_nrpm-1-3* showing phenotypes at the *er105;erl2-1* level contains *nrpm4*−/− (missing 3-bp, homozygous). Furthermore, the strong mutant *crispr_nrpm-4-1* containing *nrpm4*−/− (early termination, homozygous) is highly similar to the *er105;erl1-2;erl2-1* triple mutant, both of which exhibit severe defects in both vegetative and reproductive growth (Figures 5A and S5A).

The phenotypic resemblance between *nrpm* and *er-f* mutants inspired us to evaluate whether they are functionally connected. We generated transgenic plants expressing ERECTA-YFP driven by the native promoter in WT plants. We found that expressing an extra amount of ERECTA-YFP suppressed stomatal production in plants (Figure 5B), similar to the effect of *NRPM* overexpression (Figure 3A). When *ERECTA::ERECTA-YFP* was crossed with 35*S::NRPM3-mRFP*, we found that the stomatal phenotype was additive or synergistic, resulting in almost no stomata formation (Figure 5B). Thus, the NRPM proteins may facilitate the functions of ER-f receptor kinases at the PM and/or they function independently but converge on the same downstream regulator/s to suppress stomatal production.

Abnormal localization of ERECTA in *nrpm* mutants

It was recently reported that the subcellular dynamics of ER-f receptors are associated with their functions in specifying stomatal cell fate.[31,32] To test whether functions of NRPM are linked to the localization of ER-f receptor proteins, we examined ERECTA-YFP in *crispr_nrpm-1-3* mutants that show moderate phenotypes. As previously reported, ERECTA-YFP in *er105*[31] is predominantly localized at the PM with some internalization in leaf epidermal cells (Figure 5C; z stacked images in Figure S5B). However, this typical localization pattern of ERECTA-YFP was altered when NRPMs' activities were genetically modified (Figure 5C). ERECTA-YFP became more internalized in *crispr_nrpm-1-3* mutants (middle row, Figures 5C and S5B) but less so in *NRPM1* overexpression plants (bottom row, Figure 5C), consistently supporting a positive role of NRPM in maintaining ERECTA-YFP at the PM. However, this role does not seem to be widely applicable to other membrane receptors because the co-receptors of ERECTA, including ERL1 and SERK3, did not show changes in the localization in *crispr_nrpm-1-3* plants (Figures S5C and S5D).

To clarify the features of the ERECTA-YFP decorated membrane structures, we performed co-localization assay between ERECTA-YFP and mCherry-tagged endomembrane organelle markers, including ER-rk (CD3-959) for endoplasmic reticulum (ER),[33] Man49-mCherry (CD3-967) for Golgi,[33] mCherry-SYP61 for *trans*-Golgi network/early endosome (TGN/EE),[34] RabG3f-mCherry for prevacuolar compartments (PVCs) and tonoplast,[35] and γ-TIP-mCherry (CD3-975) for tonoplast[33] (Figures 5D–5F, S6A, and S6B). We found that ERECTA-YFP partially co-localized with the TGN/EE (Figure 5D), and largely co-localized with the markers of the PM, PVC, and tonoplast (Figures 5E and 5F). These observations were consistent with the recent discoveries suggesting that the ERECTA signaling is attenuated by U-box ubiquitin E3 ligases and ERL1 is internalized for vacuolar degradation.[31,36] To evaluate whether NRPMs participate in the vacuolar degradation pathway to regulate ERECTA, we treated plants with Wortmannin, which disturbs the endosomal maturation to form the vacuole in plant cells.[37] Indeed, we observed more prevacuolar fusions of ERECTA-YFP upon the Wortmannin treatment in WT plants, and this change was similarly induced for ERECTA-YFP in *crispr_nrpm* mutants (Figures S6C and S6D), indicating that NRPMs may not participate in the PVC maturation process.

Functional homeostasis of the PM proteins is regulated by endocytosis and endocytic recycling. In plants, brefeldin A (BFA), an ARF-GEF inhibitor, can block endocytic recycling, resulting in the membrane proteins accumulating as the "BFA-bodies."[38,39] To further investigate the effects of loss of *NRPM* on the subcellular dynamics of ERECTA, we used an endocytic tracer FM4-64 (8 μM) to stain the ERECTA-YFP seedlings for 40 min, followed by 70 μM BFA for 1 h. Results showed that the BFA treatment induced ERECTA-YFP to aggregate with FM4-64 in the BFA-bodies (Figure 5G), indicating the constant recycling of ERECTA-YFP to the PM. Furthermore, in *crispr_nrpm-1-3* mutants, more ERECTA-containing BFA-bodies were formed (Figure 5G with quantification), supporting a positive role of NRPMs in facilitating ERECTA to return to the PM. Therefore, our studies suggest that the ERECTA receptor undergoes endocytosis, followed by endocytic recycling back to the PM and vacuolar targeting for degradation, and NRPMs may promote the endocytic recycling of ERECTA to the cell surface.

NRPMs function is partially dependent on receptor signaling

The core signaling pathway regulating stomatal development involves the EPF peptide ligands, the perceiving ER-f receptors at the cell surface, and the YDA MAPK cascade in the cytoplasm, all of which are negative regulators of the key cell-fate transcription factors in stomatal production (Figure 6A). To test the genetic relationship of *NRPMs* with this pathway, we first overexpressed the peptide ligands EPF1/2 in the WT plants and *crispr_nrpm-1-3* mutants, respectively (Figures S7A and S7B).

highlighted with mCherry-tagged PIP2A, RCI2A, or NRPM1 (driven by *35S*), as indicated. Intensity profilings of YFP and mCherry were obtained along the lines drawn on the left, and internalized ERECTA-YFP signals are indicated with black arrows on the profiling. Scale bars, 20 μm.

(D–F) Co-expression of ERECTA-YFP (green) with mCherry-tagged endomembrane markers (magenta), including SYP61 (D, *trans*-Golgi network/early endosome [TGN/EE]); RabG3f (E, prevacuolar compartments and tonoplast [PVC/V]); and γ-TIP (F, vacuolar tonoplast [V]). Co-localizations were indicated by white arrows. Scale bars, 10 μm.

(G) Representative confocal images show seedlings expressing ERECTA-YFP treated with 70 μM BFA for 1 h. White arrows mark the association of ERECTA-YFP with BFA-bodies indicated by FM4-64. Histograms on the right show that more ERECTA-containing BFA-bodies formed in *crispr_nrpm-1-3* mutants. Boxes show first and third quartile with mean (line). Whiskers extend to 1 × SD from the first and third quartile. Student's unpaired t tests were used to calculate two-tailed p values. n, number of cotyledons analyzed. Scale bars, 10 μm.

See also Figures S5 and S6.

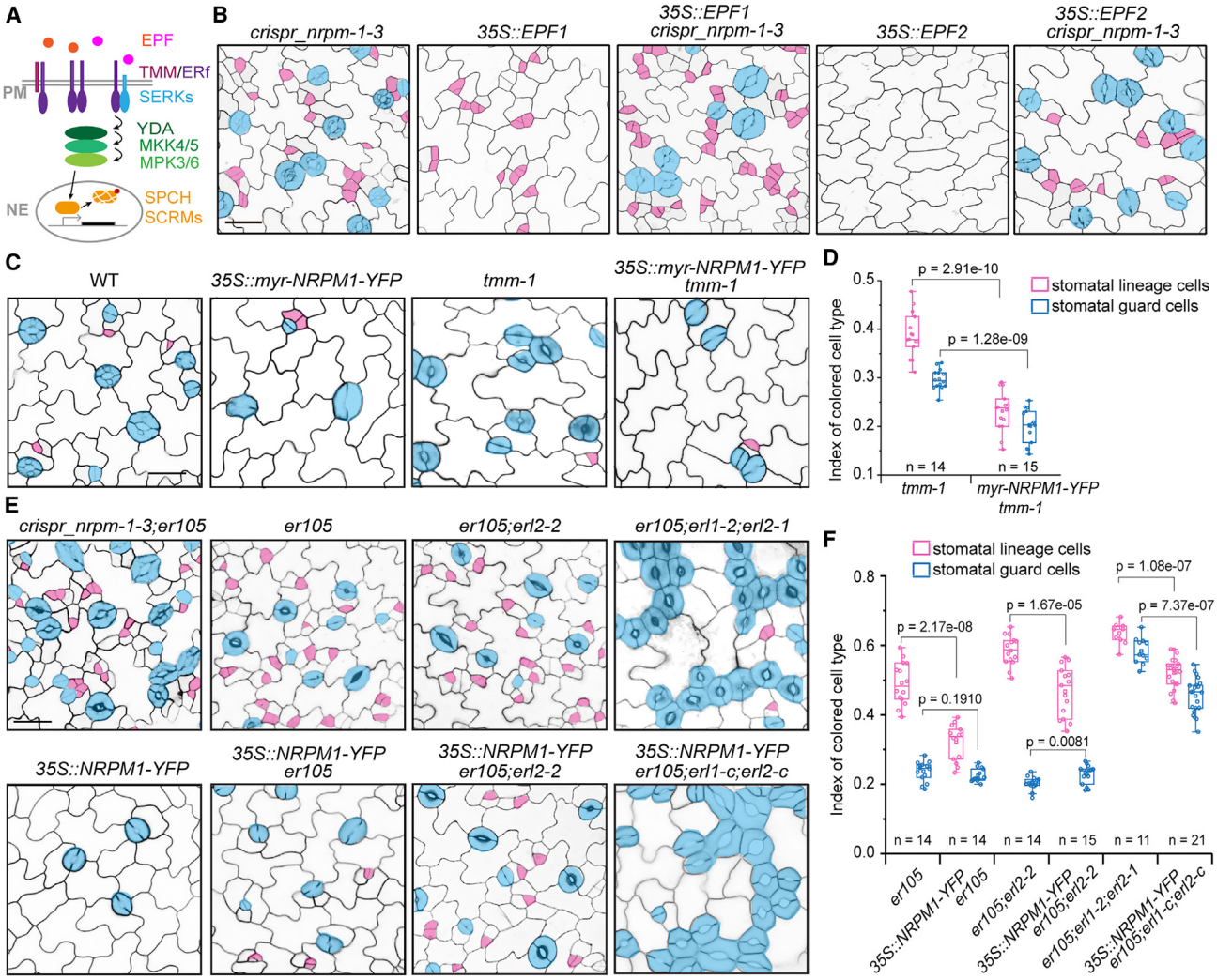

Figure 6. NRPMs function downstream of the EPF ligands and receptor/co-receptor complexes

(A) Graphic diagram describes the linear signaling pathway consisting of external peptide ligands (EPF), transmembrane receptors (TMM/ER-f, SERKs), cytoplasmic MAPK cascade (MAPKKK YDA-MAPKK 4/5-MAPK 3/6), and nuclear transcription factors (SPCH and SCRMs) in the regulation of *Arabidopsis* stomatal development. PM, plasma membrane; NE, nuclear envelope.

(B) *crispr_nrpm-1-3* is epistatic to *EPF1* and *EPF2*. Overexpression of *EPF1* and *EPF2* fails to suppress stomata formation in *crispr_nrpm-1-3* plants as in the WT background. Expression levels of *EFP1/EPF2* are provided in Figures S7A and S7B. Stomata guard cells and small dividing cells are colored in cyan and pink, respectively. Scale bars, 25 μm.

(C) Overexpression of myristoylated NRPM1 suppresses stomatal formation in *tmm-1*. *35S::myr-NRPM1-YFP* reduced stomatal formation in *tmm-1*, indicating that the TMM receptor-like protein is not required for NRPM1 to function. Scale bars, 25 μm.

(D) Quantification of stomatal and lineage index in 5-dpg cotyledons of the genotypes as indicated. n, number of cotyledons analyzed.

(E) Stomatal phenotypes of indicated genotypes. *crispr_nrpm-1-3;er105* shows additive stomata overproduction compared with *er105* or *crispr_nrpm-1-3* (see quantification data in Figure S7D). *35S::NRPM1-YFP* suppressed stomatal formation in the loss-of-function *ERECTA* receptor family, i.e., *er105* single, *er105;erl2-2* double, and *er105;erl1-c;erl2-c* triple (c, *crispr* allele, mutations shown in Figure S7C). Scale bars, 25 μm.

(F) Quantification of the stomatal phenotypes observed in the genotypes shown in (E). Boxes in (D) and (F) show the first and third quartiles with mean (square) and median (line). Whiskers extend to 1.5 × IQR from the first and third quartile. Student's unpaired t tests were used to calculate two-tailed p values. n, number of cotyledons analyzed. The methods used for the generation of combinatory genotypes are described in detail in the STAR Methods part (under "creation of genetic materials").

See also Figure S7.

Results showed that, differing from their effect of suppressing stomatal production in the WT plants, elevated expression of *EPF1/2* failed to do so in the absence of *NRPM1/2/4* (Figure 6B), indicating that NRPMs are downstream and required for the EPF-mediated signaling. This is also consistent with our results that NRPMs function inside the PM (Figures 3D and 3E), whereas the EPF peptides are apoplastic regulators.[14,15]

The ERECTA receptor-like kinase family, together with the TMM receptor-like protein and the SERKs, plays pivotal roles in suppressing stomatal formation.[16–18] In the absence of *TMM*, the

mutant plant produces more clustered stomatal GCs.[17] When the three ER-f members were progressively mutated, the stomatal overproduction phenotype became progressively severe.[19] As we found overexpression of *NRPM1* and myr-NRPM1 can suppress stomatal production (Figures 3C and 3E), we tested this regulation in the mutants carrying genetic lesions in the TMM or ER-f receptors. Results showed that myr-NRPM1 was capable of suppressing the stomatal overproduction phenotype in *tmm-1* mutants (Figures 6C and 6D). Similarly, in the loss-of-function mutants, *er105*, *er105;erl2-2*, or the newly generated *er105;erl1-c;erl2-c* triple mutant (*ERL1* and *ERL2* were knocked out by CRISPR-Cas9 in *er105*, Figure S7C), NRPM1-YFP was capable of suppressing the production of stomatal lineage cells in all these genotypes (Figures 6E and 6F). In addition, when the mutations of *crispr_nrpm-1-3* were combined with *er105*, we obtained an additive phenotype in stomatal overproduction (Figures 6E and S7D), suggesting the NRPM proteins may suppress stomatal production independent of these cell-surface receptors. However, the ability of NRPM1-YFP in suppressing stomatal lineage cells was indeed gradually attenuated with the addition of loss of *ER-f* members one by one (34.8% inhibition in *er105*, 20.1% inhibition in *er105;erl2-2*, and 17.3% inhibition in *er-f* triple mutant). Taken together, the genetic tests shown above indicate the NRPM proteins function downstream of the EPF1/2 and are likely partially dependent on ER-f kinase-mediated cell signaling in stomatal development. The fact that NRPM1 overexpression in *er-f* triple mutants maintained its activity in suppressing stomatal development also revealed its novel function independent of the ER-f receptors.

YDA is required for NRPMs to function

Downstream the cell-surface receptors, the canonical MAPK cascade, comprising the MAPKK kinase (YDA), MAPK kinases (MKK4 and MKK5), and MAPKs (MPK3 and MPK6),[9,10] acts to phosphorylate the bHLH transcription factors SPCH and SCRM/ICE1 for degradation, thereby suppresses the stomatal formation.[13,40,41] When *YDA* is absent, the leaf epidermis is predominantly covered with stomatal lineage and GCs in the super dwarf mutant plant.[9] Interestingly, this strong growth phenotype was recapitulated in some individuals among the *crispr_nrpm-1* population (Figure 7A). Inspired by this observation, we measured the MPK3/6 activity levels in *crispr_nrpm* mutants and plants overexpressing NRPM proteins. Results of immunoblotting by the p44/42 MAPK (Erk1/2) antibody indeed showed reduced MPK3/6 activities in *crispr_nrpm* and elevated activities in *NRPM*-overexpressed plants (Figures 7B and 7C), indicating a positive relationship between NRPM and the YDA MAPK pathway. To genetically test it, we overexpressed *myr-NRPM1* in *yda-3* null mutants and found that myr-NRPM failed to suppress stomatal lineage cells (Figure 7D), indicating that YDA is required for the NRPM-mediated function. On the other hand, elevated YDA activity (constitutively active YDA, YDA^{CA} driven by the *TMM* promoter) fully abolished stomatal lineage initiation and stomatal production in WT. In line with this phenotype, YDA^{CA} maintained the same activity in *crispr_nrpm-1-3* (Figure 7E). Similarly, $MKK5^{CA}$[10] or $MPK6^{CA}$[42] recapitulated the effect of YDA^{CA} in *crispr_nrpm-1-3* (Figures 7F and 7G), indicating that the YDA MAPK module functions downstream of NRPMs. In addition, the activity of SPCH transcription factor is enhanced in *crispr_nrpm-1-3* plants (Figure S7E), which is consistent with the finding that NRPMs positively regulate the YDA MAPK pathway (Figure 7B). Finally, SPCH is absolutely required for stomatal lineage initiation, regardless of the presence or absence of *NRPMs* (Figure S7F). Thus, our biochemical and genetic data suggested that the NRPM proteins function upstream of the YDA MAPK cascade to suppress stomatal production in *Arabidopsis*.

DISCUSSION

Our work identified and characterized a non-canonical HRGPs family protein of NRPM, a group of novel negative regulators of stomatal production in *Arabidopsis*. HRGPs are a class of plant cell wall proteins that contain abundant hydroxyproline residues and are often heavily glycosylated.[43] HRGPs are divided into three major subfamilies based on their protein structure and glycosylation patterns, including arabinogalactan proteins, extensins, and proline-rich proteins.[43–45] Although the NRPMs were annotated as HRGPs, they contain unknown functional domains, therefore were not enlisted in the proposed 166 HRGPs in *Arabidopsis*.[43] We also present several lines of evidence to support that NRPMs are not cell wall proteins. (1) The plasmolysis assay demonstrates that NRPMs are plasma-membrane-associated proteins (Figure 2E). (2) The myr-NRPM1 but not sp-NRPM1 maintains the function to suppress stomata formation, suggesting that NRPMs play roles from the inner side of the PM (Figures 3D and 3E). (3) None of the NRPMs has an N-terminal ER signal sequence that is one typical structure for most cell wall HRGPs.[44,45] HRGPs have been reported to play roles during signal transduction.[46,47] For example, the extracellular leucine-rich repeat extensins LRX3/4/5 function with RAPID ALKALINIZATION FACTOR (RALF) peptides RALF22/23 and receptor-like kinase FERONIA to specify a signaling pathway to response salt stress.[47] However, unlike LRXs, NRPMs neither have a leucine-rich repeat domain nor localize to the cell wall. Further research is needed to elucidate the precise mechanisms by which NRPMs associate with the inner PM and how this association contributes to signal transduction during stomatal development.

Interestingly, the *nrpm*-mutant plants exhibiting different levels of stomata and growth defects were isolated from the same CRISPR-Cas9-edited T1 plant (Figure 4A). In the meanwhile, the *nrpm*-mutant plants exhibiting comparable phenotypes but harboring different genotypes were identified from independent T1 plants (Figures 4A and 5A). These phenomena indicated that NRPMs (1/2/4) function redundantly and in a dose-dependent manner. A diverse array of weak/moderate *nrpm* alleles generated by CRISPR-Cas9 enabled us to overcome embryonic lethality and perform genetic manipulation to assay their genetic position and molecular mechanisms in different aspects of plant development and growth. In particular, the NRPM family functions upstream of YDA at the PM, leading to elevated activities of MPK3 and 6 that suppresses the differentiation of stomatal lineage cell (working model, see Figure 7H). This is based on the following key findings: (1) NRPM1 was isolated from ACD-enriched cell populations (Figure 1E) and active in stomatal lineage cells (Figures 2A, 2C, and 2D). (2) When *NRPMs* are elevated in expression, stomata formation is suppressed (Figure 3). On the other hand, loss of *nrpm* causes

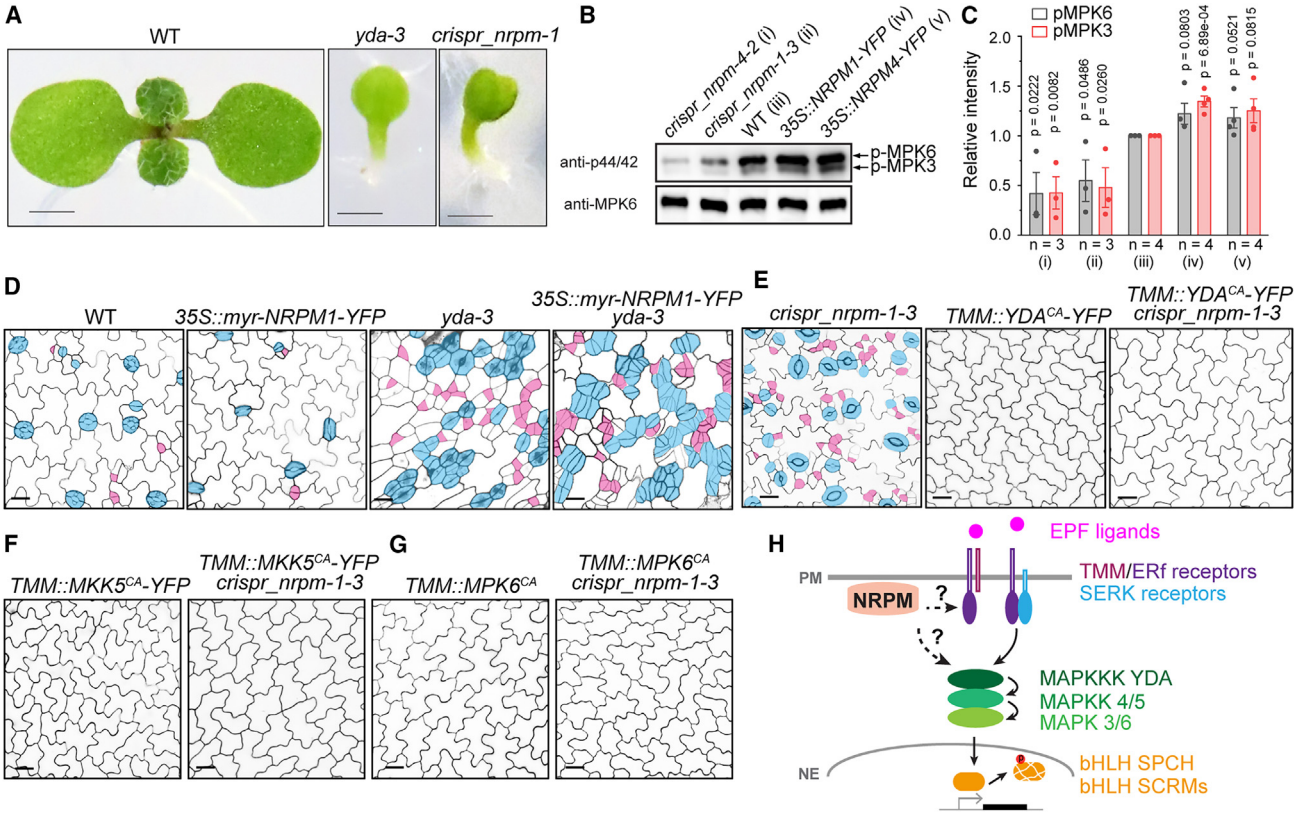

Figure 7. NRPMs function upstream of the YDA MAPK pathway

(A) Comparing growth phenotypes of a strong *crispr_nrpm-1* mutant (segregating from the T2 population of *nrpm1;2;4*) with those of a *yda-3* loss-of-function mutant (7 dpg). Scale bars, 1 mm.

(B) Representative immunoblotting data show that NRPMs positively regulate the activities of MPK3/6 *in vivo*. Anti-p42/p44 and anti-MPK6 were used to show kinase activity and protein levels of MPK6, respectively. Total proteins were extracted from 5-dpg seedlings.

(C) Quantification of MPK3/6 activity levels (p42/44) in plants with indicated genotypes in (B). The intensities of phosphorylated bands in WT were normalized to 1. Values are mean ± SD. n = 3 or 4 biological replicates.

(D–G) Confocal images show stomatal phenotypes in indicated genotypes. Images show the adaxial side of 3-dpg cotyledons. Stomata and small dividing cells are colored in cyan and pink, respectively. (D) YDA is required for the NRPM-mediated function. Overexpression of *myr-NRPM1-YFP* fails to suppress stomata formation in *yda-3* mutant. (E–G) Activation of YDA-MKK4/5-MPK3/6 MAPK cascade in stomatal lineage cells suppresses stomata formation in *crispr_nrpm-1-3* plants. Constitutively activated YDA (E), MKK5 (F), and MPK6 (G) driven by *TMM* promoter cause a stomata-less phenotype. Scale bars, 20 μm. Detailed strategies used for the generation of combinatory genotypes are described in the "STAR Methods" under "creation of genetic materials."

(H) A working model for how NRPMs function in stomata development in *Arabidopsis*. We propose that NRPMs associate the plasma membrane and function upstream of the cytoplasmic YDA MAPK pathway. Functions of NRPMs may promote the ERECTA receptor to stabilize and function at the plasma membrane directly or indirectly. NRPMs can also function independently of the ERECTA family receptors via unknown regulatory mechanisms. Activities of NRPMs at the plasma membrane lead to elevated YDA-MKK4/5-MPK3/6 signaling activity, thus lowering the amount of SPCH/SCRMs and suppressing stomatal production. The question marks denote that the pathways are unclear, which need to be further clarified.

excessive and clustered stomata (Figures 4B–4D). (3) NRPMs suppress stomata formation downstream of EPF1/2 (Figure 6B) and are partially dependent on the cell-surface ER-f receptors (Figures 6E and 6F). (4) NRPMs activate MPK3 and 6 (Figures 7B and 7C), and their roles heavily rely on the YDA-MKK4/5-MPK3/6 cascade (Figures 7D–7G). Besides YDA (MAPKKK4), NRPMs may also through MAPKKK3 and MAPKKK5, both of which regulate redundantly with YDA in plant immunity, growth, and development.[48]

Importantly, our study identified an intricate genetic interaction between NRPM proteins and the ER-f receptor kinases in both vegetative and reproductive development. The main linkage that emerged from the phenotypic and cell biological analyses appears to support the positive role of NRPM proteins in maintaining the PM homeostasis of the ERECTA receptor. This conclusion was based on the enhanced function and protein accumulation of ERECTA at the PM (Figures 5B and 5C), combined with the fact that ERECTA becomes more internalized in the *crispr_nrpm-1-3* mutants (Figures 5C and 5G). A few recent reports started revealing that the subcellular dynamics of ER-f receptors are associated with their functions in specifying stomatal cell fate.[31,32] Yang et al. reported that the protein abundance of ERECTA is reduced by the loss of *ERDJ3B* chaperon protein that causes a damaged quality control system in the endomembrane reticulum.[32] At the PM, ERECTA is activated after perceiving the EPF2 peptides, while its turnover is achieved by trans-phosphorylation of the co-receptor SERK3/BRI1-ASSOCIATED RECEPTOR KINASE 1 (BAK1) on the PUB30/31 E3 ligases,

which ubiquitinate ERECTA for eventual degradation, forming a self-organized negative feedback regulation.[36] Moreover, the co-receptor ERL1 undergoes constant internalization and recycling, demonstrating sophisticated trafficking behaviors related to the activities of upstream ligands and other receptors.[31] Here, we identified that mutations in the *NRPM* genes caused more retention of ERECTA in the endomembrane system, mainly at the PVC and vacuolar compartment (Figures 5C–5F). The BFA treatment also revealed defects of returning ERECTA to the PM in *crispr_nrpm-1-3* mutants, consistently suggesting that NRPMs help to maintain the PM localization of ERECTA. Further investigations are necessary to address several outstanding questions. For example, whether the NRPM proteins interact with ERECTA directly or indirectly? Why do NRPMs regulate the ERECTA receptor more preferentially than the other co-receptors? Though, we should not rule out the possibility that the localization or activities of the other receptor kinase can be altered in strong or null *nrpm* mutants. Eventually, how broadly are NRPMs regulating the proteins at/in the PM?

Moreover, in the absence of ER-f receptors, NRPM1 maintains the ability to suppress stomatal formation, indicating the existence of uncharacterized pathways independent of the ER-f receptors that are regulated by NRPMs at the PM. As a group of newly identified membrane-associated proteins, NRPMs deserve a significant endeavor for further characterization, given the severe developmental defects observed in the *nrpm* mutants.

STAR★METHODS

Detailed methods are provided in the online version of this paper and include the following:

- KEY RESOURCES TABLE
- RESOURCE AVAILABILITY
  - Lead contact
  - Materials availability
  - Data and code availability
- EXPERIMENTAL MODEL AND SUBJECT DETAILS
  - Plant materials and growth conditions
- METHOD DETAILS
  - Plasmid construction and plant transformation
  - Creation of genetic materials
  - RNA extraction and library preparation for RNA-seq
  - Transcriptome analysis
  - Chemical treatment
  - Plant cell imaging and image processing
  - Quantitative analysis of stomatal phenotypes in *Arabidopsis*
  - Transient expression in *N. benthamiana* epidermal cells
  - Real-time PCR
  - Examination of MPK3/6 activity in *Arabidopsis* plants
  - Accession numbers
- QUANTIFICATION AND STATISTICAL ANALYSIS

SUPPLEMENTAL INFORMATION

Supplemental information can be found online at https://doi.org/10.1016/j.cub.2024.01.052.

ACKNOWLEDGMENTS

We thank Dr. Tsuyoshi Nakagawa (Shimane University) for sharing the R4 Gateway Binary Vectors (R4pGWB). We thank Dr. Keiko Torii (The University of Texas at Austin) for sharing the seeds of *ERECTA::ERECTA-YFP;er105* (pJM284). We thank the ABRC stock center for providing the plasmids CD3-959, CD3-967, CD3-975, CD3-1007, and pX-YFP-GW, as well as the T-DNA insertional mutants. We thank the Waksman Institute Shared Imaging Facility, Rutgers, The State University of New Jersey for access to the confocal microscopes. This work was supported by grants from the National Institute of Health R01GM109080 and R35GM131827 to J.D. and start-up funds from Sanya Institute of China Agricultural University to X.X. (SYND-QDJF-02).

AUTHOR CONTRIBUTIONS

X.X. and J.D. conceived and designed this study. X.X. conducted genetic analyses. X.X., A.H., and X.G. performed immunoblotting experiments. X.X. and L.W. performed cell biological analyses. Y.S. and J.D. made the RNA libraries and deep sequencing. X.X., Z.L., and H.X. conducted transcriptomic analysis. X.X. and J.D. wrote the paper. All authors contributed to editing and approved the final manuscript. J.-K.Z. and J.D. provided funding and resources for this study.

DECLARATION OF INTERESTS

The authors declare no competing interests.

Received: April 24, 2023
Revised: October 30, 2023
Accepted: January 19, 2024
Published: February 12, 2024

REFERENCES

1. Munemasa, S., Hauser, F., Park, J., Waadt, R., Brandt, B., and Schroeder, J.I. (2015). Mechanisms of abscisic acid-mediated control of stomatal aperture. Curr. Opin. Plant Biol. *28*, 154–162.
2. Pillitteri, L.J., and Torii, K.U. (2012). Mechanisms of stomatal development. Annu. Rev. Plant Biol. *63*, 591–614.
3. Pillitteri, L.J., Sloan, D.B., Bogenschutz, N.L., and Torii, K.U. (2007). Termination of asymmetric cell division and differentiation of stomata. Nature *445*, 501–505.
4. Lampard, G.R., Macalister, C.A., and Bergmann, D.C. (2008). Arabidopsis stomatal initiation is controlled by MAPK-mediated regulation of the bHLH SPEECHLESS. Science *322*, 1113–1116.
5. Kanaoka, M.M., Pillitteri, L.J., Fujii, H., Yoshida, Y., Bogenschutz, N.L., Takabayashi, J., Zhu, J.K., and Torii, K.U. (2008). SCREAM/ICE1 and SCREAM2 specify three cell-state transitional steps leading to arabidopsis stomatal differentiation. Plant Cell *20*, 1775–1785.
6. de Zelicourt, A., Colcombet, J., and Hirt, H. (2016). The role of MAPK modules and ABA during abiotic stress signaling. Trends Plant Sci. *21*, 677–685.
7. Meng, X., and Zhang, S. (2013). MAPK cascades in plant disease resistance signaling. Annu. Rev. Phytopathol. *51*, 245–266.
8. Xu, J., and Zhang, S. (2015). Mitogen-activated protein kinase cascades in signaling plant growth and development. Trends Plant Sci. *20*, 56–64.
9. Bergmann, D.C., Lukowitz, W., and Somerville, C.R. (2004). Stomatal development and pattern controlled by a MAPKK kinase. Science *304*, 1494–1497.
10. Wang, H., Ngwenyama, N., Liu, Y., Walker, J.C., and Zhang, S. (2007). Stomatal development and patterning are regulated by environmentally responsive mitogen-activated protein kinases in Arabidopsis. Plant Cell *19*, 63–73.
11. Lampard, G.R., Lukowitz, W., Ellis, B.E., and Bergmann, D.C. (2009). Novel and expanded roles for MAPK signaling in Arabidopsis stomatal

cell fate revealed by cell type-specific manipulations. Plant Cell *21*, 3506–3517.

12. Li, H., Ding, Y., Shi, Y., Zhang, X., Zhang, S., Gong, Z., and Yang, S. (2017). MPK3- and MPK6-mediated ICE1 phosphorylation negatively regulates ICE1 stability and freezing tolerance in Arabidopsis. Dev. Cell *43*, 630–642.e4.
13. Putarjunan, A., Ruble, J., Srivastava, A., Zhao, C., Rychel, A.L., Hofstetter, A.K., Tang, X., Zhu, J.K., Tama, F., Zheng, N., and Torii, K.U. (2019). Bipartite anchoring of SCREAM enforces stomatal initiation by coupling MAP kinases to SPEECHLESS. Nat. Plants *5*, 742–754.
14. Hara, K., Kajita, R., Torii, K.U., Bergmann, D.C., and Kakimoto, T. (2007). The secretory peptide gene EPF1 enforces the stomatal one-cell-spacing rule. Genes Dev. *21*, 1720–1725.
15. Hara, K., Yokoo, T., Kajita, R., Onishi, T., Yahata, S., Peterson, K.M., Torii, K.U., and Kakimoto, T. (2009). Epidermal cell density is autoregulated via a secretory peptide, EPIDERMAL PATTERNING FACTOR 2 in Arabidopsis leaves. Plant Cell Physiol. *50*, 1019–1031.
16. Shpak, E.D., McAbee, J.M., Pillitteri, L.J., and Torii, K.U. (2005). Stomatal patterning and differentiation by synergistic interactions of receptor kinases. Science *309*, 290–293.
17. Nadeau, J.A., and Sack, F.D. (2002). Control of stomatal distribution on the Arabidopsis leaf surface. Science *296*, 1697–1700.
18. Meng, X., Chen, X., Mang, H., Liu, C., Yu, X., Gao, X., Torii, K.U., He, P., and Shan, L. (2015). Differential Function of Arabidopsis SERK Family Receptor-like Kinases in Stomatal Patterning. Curr. Biol. *25*, 2361–2372.
19. Shpak, E.D., Berthiaume, C.T., Hill, E.J., and Torii, K.U. (2004). Synergistic interaction of three ERECTA-family receptor-like kinases controls Arabidopsis organ growth and flower development by promoting cell proliferation. Development *131*, 1491–1501.
20. Velasquez, S.M., Ricardi, M.M., Dorosz, J.G., Fernandez, P.V., Nadra, A.D., Pol-Fachin, L., Egelund, J., Gille, S., Harholt, J., Ciancia, M., et al. (2011). O-glycosylated cell wall proteins are essential in root hair growth. Science *332*, 1401–1403.
21. Hijazi, M., Velasquez, S.M., Jamet, E., Estevez, J.M., and Albenne, C. (2014). An update on post-translational modifications of hydroxyproline-rich glycoproteins: toward a model highlighting their contribution to plant cell wall architecture. Front. Plant Sci. *5*, 395.
22. MacAlister, C.A., Ohashi-Ito, K., and Bergmann, D.C. (2007). Transcription factor control of asymmetric cell divisions that establish the stomatal lineage. Nature *445*, 537–540.
23. Dong, J., MacAlister, C.A., and Bergmann, D.C. (2009). BASL controls asymmetric cell division in Arabidopsis. Cell *137*, 1320–1330.
24. Zhang, Y., Wang, P., Shao, W., Zhu, J.K., and Dong, J. (2015). The BASL polarity protein controls a MAPK signaling feedback loop in asymmetric cell division. Dev. Cell *33*, 136–149.
25. Gong, Y., Alassimone, J., Muroyama, A., Amador, G., Varnau, R., Liu, A., and Bergmann, D.C. (2021). The Arabidopsis stomatal polarity protein BASL mediates distinct processes before and after cell division to coordinate cell size and fate asymmetries. Development *148*, dev199919.
26. Pillitteri, L.J., Peterson, K.M., Horst, R.J., and Torii, K.U. (2011). Molecular profiling of stomatal seristemoids reveals new component of asymmetric cell division and commonalities among stem cell populations in Arabidopsis. Plant Cell *23*, 3260–3275.
27. Kieliszewski, M.J., Lamport, D.T.A., Tan, L., and Cannon, M.C. (2011). Hydroxyproline-Rich Glycoproteins: Form and Function. Annu. Plant Rev *41*, 321–342.
28. Hallgren, J., Tsirigos, K., Pedersen, M.D., Almagro Armenteros, J.J., Marcatili, P., Nielsen, H., Krogh, A., and Winther, O. (2022). DeepTMHMM predicts alpha and beta transmembrane proteins using deep neural networks. https://doi.org/10.1101/2022.04.08.487609.
29. Magee, T., and Seabra, M.C. (2005). Fatty acylation and prenylation of proteins: what's hot in fat. Curr. Opin. Cell Biol. *17*, 190–196.
30. De Loose, M., Gheysen, G., Tiré, C., Gielen, J., Villarroel, R., Genetello, C., Van Montagu, M., Depicker, A., and Inzé, D. (1991). The extensin signal peptide allows secretion of a heterologous protein from protoplasts. Gene *99*, 95–100.
31. Qi, X.Y., Yoshinari, A., Bai, P.F., Maes, M., Zeng, S.M., and Torii, K.U. (2020). The manifold actions of signaling peptides on subcellular dynamics of a receptor specify stomatal cell fate. eLife *9*, e58097.
32. Yang, K.Z., Zuo, C.R., Leng, Y.J., Yue, J.L., Liu, H.C., Fan, Z.B., Xue, X.Y., Dong, J., Chen, L.Q., and Le, J. (2022). The functional specificity of ERECTA-family receptors in Arabidopsis stomatal development is ensured by molecular chaperones in the endoplasmic reticulum. Development *149*, dev200892.
33. Nelson, B.K., Cai, X., and Nebenführ, A. (2007). A multicolored set of in vivo organelle markers for co-localization studies in Arabidopsis and other plants. Plant J. *51*, 1126–1136.
34. Uemura, T., Ueda, T., Ohniwa, R.L., Nakano, A., Takeyasu, K., and Sato, M.H. (2004). Systematic analysis of SNARE molecules in Arabidopsis: dissection of the post-Golgi network in plant cells. Cell Struct. Funct. *29*, 49–65.
35. Cui, Y., Zhao, Q., Gao, C., Ding, Y., Zeng, Y., Ueda, T., Nakano, A., and Jiang, L. (2014). Activation of the Rab7 GTPase by the MON1-CCZ1 Complex Is Essential for PVC-to-Vacuole Trafficking and Plant Growth in Arabidopsis. Plant Cell *26*, 2080–2097.
36. Chen, L., Cochran, A.M., Waite, J.M., Shirasu, K., Bemis, S.M., and Torii, K.U. (2023). Direct attenuation of Arabidopsis ERECTA signalling by a pair of U-box E3 ligases. Nat. Plants *9*, 112–127.
37. daSilva, L.L.P., Taylor, J.P., Hadlington, J.L., Hanton, S.L., Snowden, C.J., Fox, S.J., Foresti, O., Brandizzi, F., and Denecke, J.r. (2005). Receptor Salvage from the Prevacuolar Compartment Is Essential for Efficient Vacuolar Protein Targeting. Plant Cell *17*, 132–148.
38. Geldner, N., Anders, N., Wolters, H., Keicher, J., Kornberger, W., Muller, P., Delbarre, A., Ueda, T., Nakano, A., and Jürgens, G. (2003). The Arabidopsis GNOM ARF-GEF mediates endosomal recycling, auxin transport, and auxin-dependent plant growth. Cell *112*, 219–230.
39. Naramoto, S., Otegui, M.S., Kutsuna, N., de Rycke, R., Dainobu, T., Karampelias, M., Fujimoto, M., Feraru, E., Miki, D., Fukuda, H., et al. (2014). Insights into the localization and function of the membrane trafficking regulator GNOM ARF-GEF at the Golgi apparatus in Arabidopsis. Plant Cell *26*, 3062–3076.
40. Lampard, G.R., Wengier, D.L., and Bergmann, D.C. (2014). Manipulation of mitogen-activated protein kinase kinase signaling in the Arabidopsis stomatal lineage reveals motifs that contribute to protein localization and signaling specificity. Plant Cell *26*, 3358–3371.
41. Zhao, C., Wang, P., Si, T., Hsu, C.C., Wang, L., Zayed, O., Yu, Z., Zhu, Y., Dong, J., Tao, W.A., and Zhu, J.K. (2017). MAP Kinase Cascades Regulate the Cold Response by Modulating ICE1 Protein Stability. Dev. Cell *43*, 618–629.e5.
42. Wengier, D.L., Lampard, G.R., and Bergmann, D.C. (2018). Dissection of MAPK signaling specificity through protein engineering in a developmental context. BMC Plant Biol. *18*, 60.
43. Showalter, A.M., Keppler, B., Lichtenberg, J., Gu, D., and Welch, L.R. (2010). A bioinformatics approach to the identification, classification, and analysis of hydroxyproline-rich glycoproteins. Plant Physiol. *153*, 485–513.
44. Johnson, K.L., Cassin, A.M., Lonsdale, A., Bacic, A., Doblin, M.S., and Schultz, C.J. (2017). Pipeline to Identify Hydroxyproline-Rich Glycoproteins. Plant Physiol. *174*, 886–903.
45. Johnson, K.L., Cassin, A.M., Lonsdale, A., Wong, G.K.S., Soltis, D.E., Miles, N.W., Melkonian, M., Melkonian, B., Deyholos, M.K., Leebens-Mack, J., et al. (2017). Insights into the Evolution of Hydroxyproline-Rich Glycoproteins from 1000 Plant Transcriptomes. Plant Physiol. *174*, 904–921.
46. Mecchia, M.A., Santos-Fernandez, G., Duss, N.N., Somoza, S.C., Boisson-Dernier, A., Gagliardini, V., Martínez-Bernardini, A., Fabrice, T.N., Ringli, C., Muschietti, J.P., and Grossniklaus, U. (2017). RALF4/19

peptides interact with LRX proteins to control pollen tube growth in Arabidopsis. Science *358*, 1600–1603.

47. Zhao, C., Zayed, O., Yu, Z., Jiang, W., Zhu, P., Hsu, C.C., Zhang, L., Tao, W.A., Lozano-Durán, R., and Zhu, J.K. (2018). Leucine-rich repeat extensin proteins regulate plant salt tolerance in Arabidopsis. Proc. Natl. Acad. Sci. USA *115*, 13123–13128.
48. Liu, Y., Leary, E., Saffaf, O., Frank Baker, R., and Zhang, S. (2022). Overlapping functions of YDA and MAPKKK3/MAPKKK5 upstream of MPK3/MPK6 in plant immunity and growth/development. J. Integr. Plant Biol. *64*, 1531–1542.
49. Torii, K.U., Mitsukawa, N., Oosumi, T., Matsuura, Y., Yokoyama, R., Whittier, R.F., and Komeda, Y. (1996). The Arabidopsis ERECTA gene encodes a putative receptor protein kinase with extracellular leucine-rich repeats. Plant Cell *8*, 735–746.
50. Davies, K.A., and Bergmann, D.C. (2014). Functional specialization of stomatal bHLHs through modification of DNA-binding and phosphoregulation potential. Proc. Natl. Acad. Sci. USA *111*, 15585–15590.
51. Lee, J.S., Kuroha, T., Hnilova, M., Khatayevich, D., Kanaoka, M.M., McAbee, J.M., Sarikaya, M., Tamerler, C., and Torii, K.U. (2012). Direct interaction of ligand-receptor pairs specifying stomatal patterning. Genes Dev. *26*, 126–136.
52. Cutler, S.R., Ehrhardt, D.W., Griffitts, J.S., and Somerville, C.R. (2000). Random GFP::cDNA fusions enable visualization of subcellular structures in cells of Arabidopsis at a high frequency. Proc. Natl. Acad. Sci. USA *97*, 3718–3723.
53. Lau, O.S., Davies, K.A., Chang, J., Adrian, J., Rowe, M.H., Ballenger, C.E., and Bergmann, D.C. (2014). Direct roles of SPEECHLESS in the specification of stomatal self-renewing cells. Science *345*, 1605–1609.
54. Kubo, M., Udagawa, M., Nishikubo, N., Horiguchi, G., Yamaguchi, M., Ito, J., Mimura, T., Fukuda, H., and Demura, T. (2005). Transcription switches for protoxylem and metaxylem vessel formation. Genes Dev. *19*, 1855–1860.
55. Nakagawa, T., Nakamura, S., Tanaka, K., Kawamukai, M., Suzuki, T., Nakamura, K., Kimura, T., and Ishiguro, S. (2008). Development of R4 gateway binary vectors (R4pGWB) enabling high-throughput promoter swapping for plant research. Biosci. Biotechnol. Biochem. *72*, 624–629.
56. Nakamura, S., Mano, S., Tanaka, Y., Ohnishi, M., Nakamori, C., Araki, M., Niwa, T., Nishimura, M., Kaminaka, H., Nakagawa, T., et al. (2010). Gateway Binary Vectors with the Bialaphos Resistance Gene, bar, as a Selection Marker for Plant Transformation. Biosci. Biotechnol. Biochem. *74*, 1315–1319.
57. Mcelroy, D., Chamberlain, D.A., Moon, E., and Wilson, K.J. (1995). Development of Gusa Reporter Gene Constructs for Cereal Transformation – Availability of Plant Transformation Vectors from the Cambia Molecular-Genetic Resource Service. Mol. Breed. *1*, 27–37.
58. Mao, Y., Zhang, H., Xu, N., Zhang, B., Gou, F., and Zhu, J.K. (2013). Application of the CRISPR-Cas system for efficient genome engineering in plants. Mol. Plant *6*, 2008–2011.
59. Guo, X., Ding, X., and Dong, J. (2022). Dichotomy of the BSL phosphatase signaling spatially regulates MAPK components in stomatal fate determination. Nat. Commun. *13*, 2438.
60. Schneider, C.A., Rasband, W.S., and Eliceiri, K.W. (2012). NIH Image to ImageJ: 25 years of image analysis. Nat. Methods *9*, 671–675.
61. Mi, H., Muruganujan, A., Huang, X., Ebert, D., Mills, C., Guo, X., and Thomas, P.D. (2019). Protocol Update for large-scale genome and gene function analysis with the PANTHER classification system (v.14.0). Nat. Protoc. *14*, 703–721.
62. Bray, N.L., Pimentel, H., Melsted, P., and Pachter, L. (2016). Near-optimal probabilistic RNA-seq quantification. Nat. Biotechnol. *34*, 525–527.
63. Pimentel, H., Bray, N.L., Puente, S., Melsted, P., and Pachter, L. (2017). Differential analysis of RNA-seq incorporating quantification uncertainty. Nat. Methods *14*, 687–690.
64. Warnes, G.R., Bolker, B., Bonebakker, L., Gentleman, R., Huber, W., Liaw, A., Lumley, T., Maechler, M., Magnusson, A., and Moeller, S. (2009). gplots: Various R Programming Tools for Plotting Data. R Package Version 2, 1.
65. Clough, S.J., and Bent, A.F. (1998). Floral dip: a simplified method for Agrobacterium-mediated transformation of Arabidopsis thaliana. Plant J. *16*, 735–743.
66. Llave, C., Kasschau, K.D., and Carrington, J.C. (2000). Virus-encoded suppressor of posttranscriptional gene silencing targets a maintenance step in the silencing pathway. Proc. Natl. Acad. Sci. USA *97*, 13401–13406.

STAR★METHODS

KEY RESOURCES TABLE

REAGENT or RESOURCE	SOURCE	IDENTIFIER
Antibodies		
Phospho-p44/42 MAPK (Erk1/2) (Thr202/Tyr204)	Cell Signaling Technology	Cat#9101; RRID: AB_331646
Anti-rabbit IgG, HRP-linked Antibody	Cell Signaling Technology	Cat#7074; RRID: AB_2099233
Bacterial and virus strains		
Escherichia coli TOP10	N/A	N/A
Agrobacterium tumefaciens GV3101	N/A	N/A
Chemicals, peptides, and recombinant proteins		
TRIzol	Invitrogen	Cat#15596018
SYBR Green Master Mix kit	Applied Biosystems	Cat#4309155
Protease Inhibitor Cocktail	Sigma-Aldrich	Cat#P9599
Propidium Iodide	Invitrogen	Cat#P3566
FM4-64	MedChemExpress	Cat#HY-103466
Brefeldin A	MedChemExpress	Cat# HY-16592
Wortmannin	Aladdin	Cat# W409260-1ml
Gateway LR Clonase II Enzyme mix	Invitrogen	Cat#11791100
Gateway BP Clonase II Enzyme mix	Invitrogen	Cat#11789020
Critical commercial assays		
Plant RNeasy Mini Kit	QIAGEN	Cat#74904
TruSeq RNA Sample Prep Kit v2	Illumina	Cat#RS-122-2001
SuperScrip First-Strand Synthesis System	Invitrogen	Cat#11904018
Turbo DNA-free Kit	Invitrogen	Cat#AM1907
Deposited data		
Raw and processed RNA-seq data	This study	GEO: GSE226455
Experimental models: Organisms/strains		
Arabidopsis thaliana, Col-0 ecotype (WT)	N/A	N/A
Arabidopsis nrpm1	ABRC	SALK_015461
Arabidopsis nrpm2	ABRC	SALK_127646
Arabidopsis nrpm3	ABRC	WiscDsLox501H12
Arabidopsis nrpm4	ABRC	SALK_059180
Arabidopsis nrpm1;nrpm2	This study	N/A
Arabidopsis nrpm2;nrpm4	This study	N/A
Arabidopsis nrpm1-/+;nrpm4-/+	This study	N/A
Arabidopsis spch-4	ABRC	SALK_078595
Arabidopsis yda-3	ABRC	SALK_105078
Arabidopsis tmm-1	ABRC	CS6140
Arabidopsis erl2-2	ABRC	SALK_015275
Arabidopsis basl-2	ABRC	WiscDsLox264F02
Arabidopsis er105	Torii et al.[49]	N/A
Arabidopsis er105;erl2-2	This study	N/A
Arabidopsis er105;erl1-c;erl2-c	This study	N/A
Arabidopsis er105;erl1-2;erl2-1-/+	Shpak et al.[16]	N/A
Arabidopsis SPCH::YDA^{CA}-YFP	Lampard et al.[4]	N/A
Arabidopsis 35S::SPCHΔ49	Lampard et al.[4]	N/A
Arabidopsis 35S::SPCHΔ49 basl-2	This study	N/A
Arabidopsis SPCH::SPCH-CFP	Davies and Bergmann[50]	N/A

(*Continued on next page*)

Continued

REAGENT or RESOURCE	SOURCE	IDENTIFIER
Arabidopsis ERECTA::ERECTA-YFP er105	Lee et al.[51]	pJM284
Arabidopsis 35S::GFP-PIP2A	Cutler et al.[52]	Q8
Arabidopsis ML1:mCherry-RCI2A	Lau et al.[53]	N/A
Arabidopsis 35S::NRPM1-YFP	This study	N/A
Arabidopsis 35S::NRPM2-YFP	This study	N/A
Arabidopsis 35S::NRPM3-YFP	This study	N/A
Arabidopsis 35S::NRPM4-YFP	This study	N/A
Arabidopsis NRPM1::nucYFP	This study	N/A
Arabidopsis NRPM2::nucYFP	This study	N/A
Arabidopsis NRPM3::nucYFP	This study	N/A
Arabidopsis NRPM4::nucYFP	This study	N/A
Arabidopsis NRPM1::NRPM1-YFP	This study	N/A
Arabidopsis NRPM2::NRPM2-YFP	This study	N/A
Arabidopsis NRPM3::NRPM3-YFP	This study	N/A
Arabidopsis NRPM4::NRPM4-YFP	This study	N/A
Arabidopsis NRPM1::rNRPM1-YFP	This study	N/A
Arabidopsis NRPM2::rNRPM2-YFP	This study	N/A
Arabidopsis NRPM4::rNRPM4-YFP	This study	N/A
Arabidopsis 35S::myr-NRPM1-YFP	This study	N/A
Arabidopsis 35S::sp-NRPM1-YFP	This study	N/A
Arabidopsis UBQ::Cas9/crispr_nrpm4;3;2;1	This study	N/A
Arabidopsis UBQ::Cas9/crispr_erl	This study	N/A
Arabidopsis 35S::EPF1	This study	N/A
Arabidopsis 35S::EPF2	This study	N/A
Arabidopsis 35S::NRPM3-mRFP	This study	N/A
Arabidopsis 35S::NRPM1-mCherry er105	This study	N/A
Arabidopsis TMM::YDA^{CA}-YFP	This study	N/A
Arabidopsis TMM::MKK5^{CA}-YFP	This study	N/A
Arabidopsis TMM::MPK6^{CA}	This study	N/A
Arabidopsis ERECTA::ERECAT-YFP (3002)	This study	N/A
Arabidopsis ERL1::ERL1-YFP	This study	N/A
Arabidopsis SERK3::SERK3-YFP	This study	N/A
Arabidopsis ERL1::ERL1-YFP crispr_nrpm-1-3	This study	N/A
Arabidopsis SERK3::SERK3-YFP crispr_nrpm-1-3	This study	N/A
Arabidopsis AT4G26660::nucYFP	This study	N/A
Arabidopsis AT1G53140::nucYFP	This study	N/A
Arabidopsis NRPM2::NRPM2-YFP nrpm2;nrpm4	This study	N/A
Arabidopsis crispr_nrpm-1-1	This study	N/A
Arabidopsis crispr_nrpm-1-2	This study	N/A
Arabidopsis crispr_nrpm-1-3	This study	N/A
Arabidopsis crispr_nrpm-4-1	This study	N/A
Arabidopsis crispr_nrpm-4-2	This study	N/A
Arabidopsis crispr_nrpm-6-3	This study	N/A
Arabidopsis NRPM1::rNRPM1-YFP crispr_nrpm-1-1	This study	N/A
Arabidopsis NRPM2::rNRPM2-YFP crispr_nrpm-1-1	This study	N/A
Arabidopsis NRPM4::rNRPM4-YFP crispr_nrpm-1-1	This study	N/A
Arabidopsis ERECAT-YFP (3002) x *NRPM3-mRFP*	This study	N/A
Arabidopsis NRPM1-mCherry x *ERECTA-YFP er105*	This study	N/A
Arabidopsis ERECTA-YFP er105;crispr_nrpm-1-3	This study	N/A
Arabidopsis ERECTA-YFP (3002) *crispr_nrpm-1-3*	This study	N/A

(*Continued on next page*)

Continued

REAGENT or RESOURCE	SOURCE	IDENTIFIER
Arabidopsis 35S::EPF1 crispr_nrpm-1-3	This study	N/A
Arabidopsis 35S::EPF2 crispr_nrpm-1-3	This study	N/A
Arabidopsis 35S::myr-NRPM1-YFP tmm-1	This study	N/A
Arabidopsis 35S::myr-NRPM1-YFP yda-3	This study	N/A
Arabidopsis er105;crispr_nrpm-1-3	This study	N/A
Arabidopsis 35S::NRPM1-YFP er105	This study	N/A
Arabidopsis 35S::NRPM1-YFP er105;erl2-2	This study	N/A
Arabidopsis 35S::NRPM1-YFP er105;erl1-c;erl2-c	This study	N/A
Arabidopsis TMM::YDA^{CA}-YFP crispr_nrpm-1-3	This study	N/A
Arabidopsis TMM::MKK5^{CA}-YFP crispr_nrpm-1-3	This study	N/A
Arabidopsis TMM::MPK6^{CA} crispr_nrpm-1-3	This study	N/A
Arabidopsis SPCH::SPCH-CFP crispr_nrpm-1-3	This study	N/A
Arabidopsis spch-4;crispr_nrpm-1-3	This study	N/A
Oligonucleotides		
See Table S2 for Oligonucleotides		
Recombinant DNA		
ER-RK	ABRC	CD3-959
G-RK (Man49-mCherry)	ABRC	CD3-967
VAC-RK (γ-TIP-mCherry)	ABRC	CD3-975
PM-RK (PIP2A-mCherry)	ABRC	CD3-1007
pX-YFP-GW	ABRC	6530642502
pHGY	Kubo et al.[54]	N/A
pH35GY	Kubo et al.[54]	N/A
pBGYN	Kubo et al.[54]	N/A
R4pGWB540	Nakagawa et al.[55]	N/A
pGWB654	Nakamura et al.[56]	N/A
pCAMBIA1300	Mcelroy et al.[57]	N/A
pCAMBIA2300	Mcelroy et al.[57]	N/A
pAtU6-sgRNA-pAtUBQ-Cas9	Mao et al.[58]	N/A
TMM::MPK6^{CA}	Guo et al.[59]	N/A
pENTR/D-TOPO	Invitrogen	Cat#K240020
35S::NRPM1-YFP	This study	N/A
35S::NRPM2-YFP	This study	N/A
35S::NRPM3-YFP	This study	N/A
35S::NRPM4-YFP	This study	N/A
NRPM1::nucYFP	This study	N/A
NRPM2::nucYFP	This study	N/A
NRPM3::nucYFP	This study	N/A
NRPM4::nucYFP	This study	N/A
AT4G26660::nucYFP	This study	N/A
AT1G53140::nucYFP	This study	N/A
NRPM1::NRPM1-YFP	This study	N/A
NRPM2::NRPM2-YFP	This study	N/A
NRPM3::NRPM3-YFP	This study	N/A
NRPM4::NRPM4-YFP	This study	N/A
NRPM1::rNRPM1-YFP	This study	N/A
NRPM2::rNRPM2-YFP	This study	N/A
NRPM4::rNRPM4-YFP	This study	N/A
35S::myr-NRPM1-YFP	This study	N/A

(*Continued on next page*)

Continued		
REAGENT or RESOURCE	SOURCE	IDENTIFIER
35S::sp-NRPM1-YFP	This study	N/A
UBQ::Cas9/crispr_nrpm4;3;2;1	This study	N/A
UBQ::Cas9/crispr_erl	This study	N/A
35S::EPF1	This study	N/A
35S::EPF2	This study	N/A
35S::NRPM3-mRFP	This study	N/A
35S::NRPM1-mCherry	This study	N/A
TMM::YDA^{CA}-YFP	This study	N/A
TMM::MKK5^{CA}-YFP	This study	N/A
ERECTA::ERECAT-YFP (3002)	This study	N/A
ERL1::ERL1-YFP	This study	N/A
SERK3::SERK3-YFP	This study	N/A
Software and algorithms		
ImageJ	Schneider et al.[60]	https://imagej.nih.gov
OriginPro 2022 v.9.9.0.225 (SR1)	OriginLab Corporation	https://www.originlab.com/index.aspx?go=Support&pid=4440
PANTHER v.16.0	Mi et al.[61]	http://www.pantherdb.org
KALLISTO v.0.44.0	Bray et al.[62]	https://anaconda.org/bioconda/kallisto/files?version=0.44.0
SLEUTH	Pimentel et al.[63]	https://pachterlab.github.io/sleuth/about
GPLOTS	Warnes et al.[64]	https://rdrr.io/cran/gplots/
Other		
StepOnePlus Real-Time PCR System	Applied Biosystems	Cat#4376598
Nanodrop spectrophotometer	Thermo Fisher	Cat#ND-ONEC-W
Agilent 2100 Bioanalyzer	Agilent Technologies	Cat#G2939BA

RESOURCE AVAILABILITY

Lead contact

Further information and requests for resources and reagents should be directed to and will be fulfilled by the lead contact, Juan Dong (dong@waksman.rutgers.edu).

Materials availability

All plasmids and *Arabidopsis thaliana* lines generated in this study are available from the lead contact upon request.

Data and code availability

- Raw RNA-seq data have been deposited on NCBI's Gene Expression Omnibus (GEO) under the project number GSE226455.
- No original code is reported in this study.
- Additional information required to reanalyze the data reported in this paper is available from the lead contact upon request.

EXPERIMENTAL MODEL AND SUBJECT DETAILS

Arabidopsis (*Arabidopsis thaliana*) plants are in the Columbia (Col-0) background as described in the key resources table. *Arabidopsis* and tobacco *Nicotiana benthamiana* were grown in controlled growth conditions, as described in method details.

Plant materials and growth conditions

The *Arabidopsis thaliana* ecotype Columbia (Col-0) was used as the wild-type unless otherwise noted. Seeds were surface sterilized with 70% ethanol for 5 min, rinsed three times with autoclaved distilled water. After 3-day imbibition in the dark at 4 °C, seeds were sown on half-strength Murashige & Skoog medium with 1% agar (A1296, Sigma), pH 5.8. Seeds germinate in a growth chamber under 16-h light/8-h dark cycle with 100 μmol m^{-2} s^{-1} light intensity at 22 °C. The 7-day-old seedlings were transferred to the soil

for further growth under the same conditions. The *Nicotiana benthamiana* plants were grown in a growth room at 25°C under 14-h light/10-h dark cycle. The plasmid CD3-1007 (*35S::PIP2A-mCherry*)[33] and T-DNA insertional lines *nrpm1* (SALK_015461), *nrpm2* (SALK_127646), *nrpm3* (WiscDsLox501H12), *nrpm4* (SALK_059180), *erl2-2* (SALK_015275), and *spch-4* (SALK_078595) were obtained from *Arabidopsis* Biological Resource Center (ABRC). *basl-2* (WiscDsLox264F02),[23] *ML1:mCherry-RCI2A*,[53] *35S::GFP-PIP2A*,[52] *TMM::MPK6*^{CA},[59] *er105*,[49] *er105;erl1-2;erl2-1*,[16] *ERECTA::ERECTA-YFP er105* (pJM284),[51] *SPCH::SPCH-CFP*,[50] and *35S::SPCHΔ49*[4] were described previously.

METHOD DETAILS

Plasmid construction and plant transformation

NRPM coding sequence (CDS) were amplified using Q5 high fidelity DNA polymerase (NEB), and then were inserted into JW819-VENUS (pCAMBIA3300 backbone) by TA cloning to make 35S::NRPMs-VENUS. In order to facilitate the subsequent vector construction, we switched to LR Clonase II (Invitrogen)-based gateway cloning technology for more constructions. NRPM encoding regions with stop codons removed were cloned into pENTR/D-TOPO (Thermo Fisher Scientific) through NotI and AscI sites, and then the promoters were inserted at NotI site immediately upstream of the coding sequences. The plasmid pENTR/D-TOPO carrying the *NRPM* coding region were recombined into pX-YFP-GW to make *35S::NRPMs-YFP*, or into pGWB654[56] to make *35S::NRPMs-mRFP*. The plasmid pENTR/D-TOPO carrying the *NRPMp::NRPM* were recombined into pHGY[54] to generate *NRPMp::NRPM-YFP*. The CRISP/Cas9 resistant version of NRPMs (rNRPMs) were generated through two round PCR to introduce the synonymous mutation in the Cas9-gRNA recognition site. The same method was used to make *NRPM::rNRPMs-YFP*, *ERECTA::ERECTA-YFP* (3002), *ERL1::ERL1-YFP*, and *SERK3::SERK3-YFP* in pHGY backbone. Briefly, the genomic coding sequence of genes was amplified and cloned into pENTR/D-TOPO by NotI and AscI. Then promoter region was inserted by the NotI site before the coding sequence. NRPM promoters were cloned into pENTR/D-TOPO through NotI and AscI sites. The pENTR/D-TOPO carrying *NRPM* promoters were recombined into pBGYN[54] to make *NRPMp::nucYFP*.

To make *35S::myr-NRPM1-YFP* and *35S::sp-NRPM1-YFP*, the *NRPM1* coding region was cloned into pENTR/D-TOPO via NotI and AscI, while introducing a KpnI site immediately upstream of the coding sequences. Then *myr* was inserted via NotI and KpnI sites to make pENTR/D-TOPO/myr-NRPM1. The *myr* was replaced by the signal peptide of Extensin 3 (AT1G21310) to make pENTR/D-TOPO/sp-NRPM1. Finally, through LR reaction, the entry vectors and pH35GY were recombined to obtain *35S::myr-NRPM1-YFP* and *35S::sp-NRPM1-YFP*.

To make *35S::EPF1/2*, the genomic sequence of *EPF1* and *EPF2* were amplified and inserted into pCAMBIA1300/35S::MCS::NOS via BamHI and KpnI. The CaMV 35S promoter, NOS terminator, and multiple clone sites (MCS) between them have been pre-installed on the pCAMBIA1300[57] backbone by HindIII and EcoRI.

The *TMM* promoter was cloned into pDONR-P4-P1R (Thermo Fisher Scientific) via BP reaction. The pENTR/D-TOPO containing *YDA*^{CA} and *MKK5*^{CA} with stop codons removed were reported previously.[11] Double LR recombination reactions were performed to integrate pENTR/D-TOPO containing YDA^{CA} or MKK5^{CA} and pDONR-P4-P1R/TMMp into the R4pGWB540[55] to make *TMM::YDA*^{CA}*-YFP* and *TMM::MKK5*^{CA}*-YFP*, respectively.

To create CRISPR/Cas9-mediated mutagenesis in *Arabidopsis*, we adopted the system described in a previous study.[58] Following the introduction, the oligos NRPM4-CRI-F and NRPM4-CRI-R were phosphorylated by T4 PNK (NEB) and annealed in a thermocycler. The annealed oligos were cloned into the plasmid pAtU6-sgRNA-pAtUBQ-Cas9 via BbsI site. The same procedure was performed to create other three guide RNA cassettes. The chimeric pAtU6- NRPM4-pAtUBQ-Cas9 cassette was cut off and subcloned into pCAMBIA2300[57] through HindIII and EcoRI sites to get 2300/crispr_nrpm4. U6-NRPM3 was amplified by PCR and inserted into 2300/crispr_nrpm4 through KpnI and EcoRI sites to get 2300/crispr_nrpm4;3. Using same strategy, U6-NRPM2 were inserted at KpnI site to create the construct 2300/crispr_nrpm4;3;2 and finally U6-NRPM1 were inserted at EcoRI site to create the construct 2300/crispr_nrpm4;3;2;1 to knock-out the whole family. Same strategy as building 2300/crispr_nrpm4, one single guide RNA targeting both ERL1 and ERL2 was cloned into pCAMBIA1300 to make 1300/crispr_erl. See also Table S2 for the primers used in this study.

The plasmids were transformed into *Agrobacterium tumefaciens* GV3101, which were used for stable transformation in *Arabidopsis* and transient expression in *N. benthamiana*. *Arabidopsis* plants were transformed with the standard floral dipping method,[65] and the T0 seeds were subjected to antibiotic selection.

Creation of genetic materials

35S::SPCHΔ49 had been reported previously[4] and was crossed with *basl-2* mutant to obtain *35S::SPCHΔ49;basl-2*. The construct containing CRISPR/Cas9 targeting NRPMs was introduced to Col-0 plants expressing *ML1::mCherry-RCI2A* (WT) to create *crispr_nrpm* mutants. Stable *crispr_nrpm-1-1* and *crispr_nrpm-1-3* with moderate fertility defects were isolated from the *crispr_nrpm-1* population and used for further genetic analysis. The *rNRPM* constructs were introduced to *crispr_nrpm-1-1* by dipping and the representative plants are shown in Figure 4. The mCherry-tagged endomembrane organelle markers were introduced to *ERECTA::ERECTA-YFP;er105* by dipping except RabG3f-mCherry by crossing.

For genetic interaction assay, especially the combinations of overexpression cassettes with mutants, we follow this principle: at least two independent overexpression lines were chosen to cross with mutants, and then the desired plants were isolated from the F2 or F3 population by genotyping. Due to some technical difficulties, a few exceptions are described here. 1) *35S::EPF1/2* were introduced into *crispr_nrpm-1-3* and WT, respectively. Several T1 plants in WT background showing stomata-less phenotypes

at the early stage (5-dpg), indicating our constructs work. But among over 120 T1 seedlings in *crispr_nrpm-1-3* background we examined, none shows stomata-less phenotypes. To ensure the same transgenic alleles in both WT and *crispr_nrpm-1-3* background, several independent T1 plants in *crispr_nrpm-1-3* background (father) were crossed with Col-0 (mother). The stomata-less seedlings at 3-dpg were isolated from the F1 population, then images were captured from the corresponding father lines and stomata-less F1 plants, which were represented in Figure 6B; 2) The material *35S::NRPM1-YFP er105;erl1-c;erl2-c* was created by introducing CRISPR/Cas9 targeting *ERL1/2* into *35S::NRPM1-YFP er105* background by dipping; 3) *TMM::YDA^{CA}-YFP*, *TMM::MKK5^{CA}-YFP*, and *TMM::MPK6^{CA}* were introduced to *crispr_nrpm-1-3* by dipping because YDA^{CA}, MKK5^{CA}, and MPK6^{CA} cause stomata-less phenotype in WT background.

RNA extraction and library preparation for RNA-seq

Total RNA was isolated from 12-day-old *Arabidopsis* seedlings with the RNeasy Plant Mini Kit (Qiagen, Germany) following the manufacturer's instructions. RNA quantification was measured with a Nanodrop spectrophotometer (Thermo Fisher Scientific, USA) and the integrity of RNA was examined with the Agilent 2100 Bioanalyzer (Agilent Technologies, USA). RNA samples with RNA integrity number more than 7.0 were used for library preparation. The RNA-seq libraries were prepared at the Core Facility for Genomics at Shanghai Center for Plant Stress Biology using the Illumina TruSeq RNA Sample Prep Kit v2 LS protocol (Illumina, USA) and then sequenced on Illumina HiSeq2000 platform.

Transcriptome analysis

The transcript levels were quantified using KALLISTO v.0.44.0[62] by mapping to *Arabidopsis* (genome release version 11) primary transcript sequences. Differentially expressed genes (DEGs) were identified using SLEUTH[63] as those showing $|b| \geq 0.692$ and q-value < 0.05 with transcript per million (TPM) reads counts over 10 in one group at least. Hierarchical clustering was performed using GPLOTS[64] in R based on the TPM data for DEGs. Gene ontology (GO) enrichment analysis was performed using PANTHER v.16.0[61] with significant P-values ($P < 0.05$) to export the top GO terms.

Chemical treatment

All chemical treatments were performed on 3-dpg *Arabidopsis* seedlings. Treatment after a certain period of time as described in the main text, the seedlings were mounted for confocal imaging. For internalization assay, ERECTA-YFP seedlings were incubated with 8 μM FM4-64 for 40 mins before imaging. For BFA treatment, seedlings were stained with 8 μM FM4-64 for 40 mins, followed by 1-hr treatment with 70 μM BFA. For wortmannin treatment, FM4-64 staining was followed by treatment with 33 μM wortmannin for 3 hrs.

Plant cell imaging and image processing

Confocal images of plant cells expressing fluorescence-tagged proteins were taken on a Leica SP5 confocal microscope. The 3-day-old adaxial side of cotyledons was captured. Cell outlines were visualized by propidium iodide (PI, Invitrogen). Seedlings were stained in PI solution (1:100 diluted) for 12-15 min. Fluorescence was excited at 514 nm (YFP) and 594 nm (PI). Emissions were collected at 520-540nm (YFP) and 620–640 nm (PI). The confocal images were false-colored, and brightness/contrast were adjusted using either Adobe Photoshop 23.1.0 or ImageJ.[60] To present stomata patterning clearly, images with cell outlines decorated by PI or YFP signals were converted to black and white, and then stomata and small dividing cells were colored in cyan and pink, respectively.

Quantitative analysis of stomatal phenotypes in *Arabidopsis*

The adaxial cotyledons of 5-day-old *Arabidopsis* seedlings were stained with propidium iodide (Invitrogen), and images were captured using a Carl Zeiss Axio Scope A1 fluorescence microscope equipped with a ProgRes MF CCD camera (Jenoptik). The Stomata index or stomatal lineage cells index was calculated as the number of stomata or stomatal lineage cells versus the total number of epidermal cells.

Transient expression in *N. benthamiana* epidermal cells

For the method of transiently expressing genes in *N. benthamiana*, we made some modifications based on a previous report.[66] *Agrobacterium tumefaciens* GV3101 harboring the plasmids of *35S::NRPMs-YFP* were cultured overnight in 10 ml Luria broth medium containing appropriate antibiotics at 30°C. Bacterial cells were collected at 10,000 rpm for 1 min and resuspended with 10 ml water to wash out the antibiotics, followed by one more time washing. Then cells were resuspended in the infiltration buffer (10 mM $MgCl_2$, 10 mM MES pH 5.7, 200 μm acetosyringone) and the cell concentration was adjusted to $OD_{600} = 0.8$. Cells were placed in culture medium for 2 hours at room temperature prior to infiltration. By using a 1-ml syringe, the Agrobacterium solution was infiltrated into leaves through an incision. At third-day post-infiltration, the fluorescence on the epidermis was observed and images were captured on a Leica SP5 confocal microscope.

Real-time PCR

Total RNAs were extracted from 3-day-old seedlings using TRIzol (Invitrogen). DNA was digested with the Turbo DNA-free Kit (Invitrogen). The first-strand cDNAs were synthesized by the SuperScrip First-Strand Synthesis System (Invitrogen) using 1 μg total RNAs as templates in a volume of 20 μl. Real-time PCR was performed with a SYBR Green Master Mix kit (Applied Biosystems) and

amplification was monitored on a StepOnePlus Real-Time PCR System (Applied Biosystems). The gene expression level was normalized to reference gene *S18C* (*AT4G09800*) using the ΔCT method. Primers are listed in Table S2.

Examination of MPK3/6 activity in *Arabidopsis* plants

To evaluate the MAPK activity, 5-day-old seedlings were frozen in liquid nitrogen and homogenized by pestles. Total proteins were extracted in a buffer containing 100 mM HEPES (pH7.5), 5 mM EDTA, 5 mM EGTA, 10 mM NaF, 10 mM Na_3VO_4, 50 mM β-glycerophosphate, 5% glycerol, 10 mM DTT, 1 mM PMSF and 1% protease inhibitor cocktail for plant cell extracts (Sigma-Aldrich). After centrifugation at 13,000 rpm for 15 min, supernatants were transferred to new tubes. Equal amounts of total protein were loaded and separated from each other based on their size by the electrophoresis on a 12% SDS-PAGE gel. The MAPK activity was determined by immunoblotting with the primary antibody against Phospho-p44/42 MAPK (Erk1/2) (Thr202/Tyr204) (1:1000, Cell Signaling Technology). Equal loading was indicated by immunoblot analysis with anti-MPK6 antibody.

Accession numbers

NRPM1 (AT4G25620), NRPM2 (AT5G52430), NRPM3 (AT1G63720), NRPM4 (AT1G76660), SPCH (AT5G53210), BASL (AT5G60880), EXT3 (AT1G21310), ERECTA (AT2G26330), ERL1 (AT5G62230), ERL2 (AT5G07180), SERK3 (AT4G33430), TMM (AT1G80080), YDA (AT1G63700), MKK5 (AT3G21220), MPK6 (AT2G43790), MPK3 (AT3G45640).

QUANTIFICATION AND STATISTICAL ANALYSIS

Differentially expressed genes (DEGs) were identified using SLEUTH.[63] Gene ontology enrichment analysis was performed using PANTHER v.16.0.[61] All boxplots show the range from first to third quartile with mean (square) and median (line). Whiskers extend to 1.5 x IQR from first and third quartile. Data points outside the whiskers were considered outliers. Column bar plots show the mean values with standard errors. Statistical analysis of quantitative data were performed using OriginPro 2022 v.9.9.0.225 (SR1) or Microsoft Excel. A two tailed *t*-test was used for comparisons between two groups. One-way ANOVA and Tukey's method were used for multiple comparisons. Significance was defined as P value < 0.05.